NIPER-472
April 1990

NIPER
Commitment to Excellence

STATUS REPORT

SELECTION OF A SECOND BARRIER ISLAND RESERVOIR SYSTEM FOR EXPANDING THE SHORELINE BARRIER RESERVOIR MODEL AND REFINING NIPER RESERVOIR CHARACTERIZATION METHODOLOGY

By Michael Szpakiewicz, R. Schatzinger,
S. Jackson, B. Sharma, A. Cheng, and
Matt Honarpour

Work Performed for the
U.S. Department of Energy
Under Cooperative Agreement DE-FC22-83FE60149

National Institute for Petroleum and Energy Research
IIT Research Institute • P.O. Box 2128
Bartlesville, Oklahoma 74005 • (918) 336 - 2400

NIPER-472
Distribution Category UC-122
April, 1990

STATUS REPORT

SELECTION OF A SECOND BARRIER ISLAND RESERVOIR SYSTEM FOR EXPANDING THE SHORELINE BARRIER RESERVOIR MODEL AND REFINING NIPER RESERVOIR CHARACTERIZATION METHODOLOGY

Project BE1, Milestone 1, FY90

by

By Michael Szpakiewicz, R. Schatzinger, S. Jackson, B. Sharma, A. Cheng and M. Honarpour

Work Performed for
Department of Energy
Under Cooperative Agreement
DEFC22-83FE60149

Edith Allison, Project Manager
Department of Energy
Bartlesville Project Office

IIT Research Center
National Institute for Petroleum and Energy Research
P. O. Box 2128
Bartlesville, Oklahoma

TABLE OF CONTENTS

TABLES

ILLUSTRATIONS

SELECTION OF A SECOND BARRIER ISLAND RESERVOIR SYSTEM FOR EXPANDING THE SHORELINE BARRIER RESERVOIR MODEL AND REFINING NIPER RESERVOIR CHARACTERIZATION METHODOLOGY

By

M. Szpakiewicz, R. Schatzinger, S. Jackson, B. Sharma, A. Cheng and M. Honarpour

---

ABSTRACT

Generalization of shoreline barrier reservoir characteristics is a primary objective of the BE1 project, "Reservoir Assessment and Characterization." The Upper Cretaceous Almond formation in Patrick Draw oil field, southwestern Wyoming, has been selected from 18 primary candidates for comparison with the Lower Cretaceous Muddy formation in Bell Creek field, southeastern Montana. Both oil productive reservoirs selected for broadening geological and engineering understanding of the system represent a combination of "end-member" models of shoreline barriers developed under different hydrodynamic conditions. The hydrodynamic conditions primarily involve changes in sea level and the dominant tide and wave regime of a coastline.

The productive Muddy formation in Bell Creek predominantly consists of fine-grained littoral and neritic sandstones deposited as shoreface and foreshore facies in a shoreline barrier system, whereas the Almond formation in Patrick Draw contains two distinct units consisting of fine - to medium - grained estuarine sandstones deposited in a tidal channel/tidal delta environment asociated with migrating a tidal inlets within a barrier-island coastline and some fine to very fine-grained littoral and shallow neritic sandstones. For broadening comparative aspects of these oil-productive shoreline barrier systems, geologic information on a number of well documented outcrops and several representatives of the Holocene barriers have also been collected.

Studied similarities and contrasts of the two types of ancient oil-producing shoreline barrier deposits will indicate the extent to which coastal barriers can be generalized in a meaningful manner. By comparing the barrier island model developed to that for Patrick Draw field, the resulting model will become more broadly applicable. A spectrum of geologic and engineering data are being collected from Patrick Draw field and analyzed to reach that goal.

OBJECTIVES OF THE PROJECT

The overall objective of NIPER's Reservoir Characterization Program is to develop a better understanding of the influence of deposystem-specific reservoir heterogeneities on the movement and trapping of fluids. A quantitative geological/engineering model has been constructed and used to evaluate the influence of heterogeneities on primary, secondary, and tertiary production. An integrated methodology for constructing a quantified hydrodynamic model for application to barrier island reservoirs was developed based on Bell Creek (MT) field, and nearby analogous outcrops. Selection of a second shoreline barrier/barrier island reservoir for characterization was an integral part of this project.

The task to meet these objectives (milestone 1, FY90 Annual Research Plan) was to select a second barrier island system (a) to test the reservoir characterization methodology, (b) to generalize the geological/engineering model for barrier island reservoirs, and (c) to improve the predictability of barrier island reservoir production performance based on the geological/engineering model. With the selection of Patrick Draw field, milestone 1 has been completed.

INTRODUCTION

Prior to the 1970s, the prograding Galveston Island depositional model was considered by many geologists as the "one and only" facies model for interpreting ancient barrier-island sequences. Studies conducted within the past 20 years indicate that the use of one normative model is unrealistic.[1] Three generalized facies models or end-member to barrier island sequences can be recognized: (1) regressive barrier, (2) transgressive barrier, and (3) barrier-inlet[1] (see figure 1). Most ancient shoreline barrier sequences can be classified through comparative analyses with individual "end-member" models or a combination of them.

The previously studied Muddy formation in Bell Creek (MT) field and analogous Muddy formation outcrops in NE Wyoming (New Haven area) consist of a dominantly regressive (prograding) sequence of facies with minor elements from a transgressive event at the base of the sequence.[2-3] Thus to broaden the range of studied end-members for barrier island reservoir characterization (Task 1 of Project BE1, FY90) and to make the geological/engineering model more broadly applicable to a wider range of reservoirs, our attention was drawn to the selection of reservoirs where barrier island and associated tidal inlet sequences of facies dominate in productive intervals.

PROCESS FOR SELECTING A SECOND SHORELINE BARRIER RESERVOIR SYSTEM

Initial Candidates

Eighteen candidates were chosen (table 1). A shoreline barrier literature data base has been continually updated and now contains the collected references about the Almond formation, Patrick Draw field, stratigraphy, sedimentology and petrography of barrier sediments, and references about the formations and specific fields considered. (See appendix A). A review of these cases indicated that a similar spectrum of facies occurs in most barrier systems. The variations of processes, however, control the predominance of the various facies. For example, in mesotidal deposition, tidal processes dominate and tidal inlet, tidal channel, and tidal delta facies are predominant, whereas in a microtidal system marine processes dominate and foreshore, shoreface, and washover facies are predominant. The extensive search of the literature was supplemented by discussions with consultants and specialists in industry, visits to core repositories, and examinations of cores from various sources.

The following criteria were established for selection of a second reservoir:

1. The reservoir must comprise a shoreline barrier that will expand the model developed based on Bell Creek field.
2. It should be a prolific oil producer (OOIP>100 MM STB).
3. A complete suite of geological and engineering data from the reservoir should be available to NIPER.
4. Nearby analogous outcrops should be available.
5. The reservoir should have a history of some primary and secondary production and should be a potential EOR candidate.
6. The reservoir should be in the continental U.S. , preferably within the Rocky Mountain Region.

Based upon the above criteria, the number of candidate reservoirs was reduced. A list of the top five candidate reservoirs and a comparative summary of their reservoir properties with Bell Creek field are shown in tables 2 and 3. Because shoreline barriers comprise a variety of genetic types,[4] it was necessary to know which type of barrier the candidates represented. It was also important to select a reservoir which is at a comparable stage of oil recovery with Bell Creek. The reported environments of deposition are, therefore, summarized along with some other important parameters for each of the top five candidate reservoirs (tables 2 and 3).

Sandbodies that are originally detached from the strandplain may through time become connected to the mainland by vertical accretion on the lee side of the barrier, or by bay-head delta progradation. An example is provided by the Upper Cretaceous Gallup Sandstone within the San Juan Basin where a lagoon became a coal swamp and the associated barrier island (senso stricto) became attached to the mainland as the swamp replaced the lagoon (Campbell, 1979).[5] Such sequences that record the vertical (and therefore temporal) shift from detached shorelines to attached shoreline sands actually may be very common and play an important role in development and growth of strandplains and chenier plains such as seen on the Gulf Coast. Knowledge of this natural complexity in the relationship between attached and detached, submerged and emergent shoreline barriers meant that the search for barrier island reservoir settings in the strict sense must be de-emphasized. Instead, more emphasis was placed on determining the type of shoreline barrier candidates represented and whether they would be the best reservoir for comparing and contrasting the setting of Unit 'A' at Bell Creek and for testing the reservoir characterization methodology.

Outcrop exposures and modern environments provide extremely useful information about geometry and lateral extent of facies for developing shoreline barrier models. Information on a number of well documented outcrops (table 4) and several representative modern shoreline barriers (table 5) were collected and may be considered for future use in shoreline barrier model developments.

Ranking of Top Five Candidate Reservoirs

The top five candidate reservoirs of 18 which were considered are summarized in tables 2 and 3. At this time, the first candidate reservoir is Patrick Draw field, located on the east side of the Rock Springs Uplift, Greater Green River Basin, Wyoming. Barrier-related production is from the Upper Almond formation, between 4,000 and 5,000 ft below surface. The reported depositional environment is barrier island (probably prograding) and associated inlet fill.[6] Patrick Draw field was selected as first choice because it fulfills the criteria established to meet the objectives of the project (listed above) more than any of the other reservoirs. In addition, consultants Rod Tillman and Bob Weimer have previously been involved with subsurface and outcrop geological studies of Patrick Draw field and vicinity and are both willing to be of assistance.

The second candidate was Hilight field producing from the Muddy formation in Powder River Basin, south of Bell Creek field. The barrier island sandstones are the most prolific producers there, followed by the underlying fluvial and delta front sandstones (Wheeler et al. 1988).[10] Analyses of facies and facies sequences in cores from Hilight field provide direct lithologic evidence of depositional paleoenvironments, but cannot reliably distinguish between some paleoenvironments with similar deposits; e.g. wave-dominated delta front vs. shoreface, or lagoon vs. bay.[10] The top-most sandstone interval--Springer Ranch Member--is interpreted as progradational barrier island/spit and tidal inlet deposits.

The third rated choice was West Ranch field, which produces from the Oligocene Frio formation between 5,100 and 5,700 ft in the Texas Gulf Coast. This large field contains three barrier intervals developed under microtidal regime and classified as aggrading, transgressive, and progradational barrier islands (Galloway, 1986).[7] The three producing intervals are responsible for an estimated 499 million barrels OOIP. Unfortunately the amount of core available from these intervals is questionable. Much of the known core was unconsolidated and has become disaggregated.[8] Ranking of this reservoir was also somewhat lowered because it is not located within the same general geological province (Rocky Mountain region) as was the first study at Bell Creek.

The fourth candidate was Elk City field, which produces from relatively deep (9,400 ft) Pennsylvanian sandstones in the Anadarko Basin of southwestern Oklahoma. This field is reported to produce from deltaic and associated barrier bar deposits. The type of bar remains unclear at this time, and it is uncertain whether the barrier portion accounts for more than 10% of the reservoir.

The fifth candidate reservoir was Bisti field which produces from the Gallup sandstone in the San Juan Basin of northwestern New Mexico. Based on the recent literature (Tillman, 1985),[9] the depositional environment for Bisti field does not appear to meet the requirements for a shoreline barrier.

In addition to the five reservoirs listed in tables 2 and 3, two cores from the Almond formation at Sun Ranch (TX) field, operated by Oryx Oil Co., were studied during a trip to the offices of Oryx in Dallas, TX. One of the cores was too tight for consideration and barrier facies could not be identified in the other core. A third Oryx core was sent to NIPER for analysis. The objective at this time is to conduct a CT scan of this core and then perform a fractal analysis of the recorded electron density profile as part of milestone 4 of Project BE1, to determine anisotropy related to bedding.

Almond Formation/Patrick Draw Field-Selected

Of the five reservoirs that showed the greatest potential for a comparative study and test of the developed reservoir characterization methodology, Patrick Draw field is the highest rated candidate and has been selected. Therefore, somewhat more detailed descriptions of the advantages/disadvantages of the reservoir and geological characteristics are presented.

Advantages/Disadvantages of Almond Formation/Patrick Draw Field

The advantages include the following:

1. Reservoir location. This field is located within a similar geographic area (Rocky Mountain region) as was the reservoir in the previous work. Similarities between the reservoirs include geological province, age of the formation, and tectonic regime although Patrick Draw is located in a different basin (Powder River vs Green River basins). These similarities would allow meaningful comparisons of the two sandbodies. In addition, our expertise in the Rocky Mountain region will facilitate the collection and interpretation of data and the determination of similarities and differences between the two reservoirs.

2. Extensive outcrop exposure. Outcrops of the upper Almond formation exist within 10 miles of the subsurface production in Patrick Draw field (fig. 2) More than 100 miles of outcrop are available along the Rock Springs Uplift which exposes a barrier island 60 miles long and 4 miles wide (Rochler, 1988).[11]

3. Available cores and logs. More than 80 cores from the Arch Unit of Patrick Draw field are available from the USGS core repository for analysis.

4. Variation of shoreline barrier type. The Almond formation represents a different "end-member" of barrier/island deposition (fig. 1) compared to the Muddy formation in Bell Creek field. Although both formations were deposited in a shoreline barrier setting, the low tidal range during Muddy deposition (microtidal) resulted in long, laterally uninterrupted barrier core sand bodies. In contrast, the higher tidal range during Almond deposition (mesotidal) produced short, drumstick-shaped barriers (Flores, 1978).[6] The Almond deposits are complicated with a mosaic of associated barrier system facies such as tidal deltas and tidal creek channels.

The similarities and contrasts of these two types of barrier shoreline deposits will indicate the extent to which coastal barriers can be generalized in a meaningful manner. By adding models of Patrick Draw field to that developed for Bell Creek field, the model will become more broadly applicable to other barrier fields.

The disadvantages include the following:

1. The reservoir thickness within Patrick Draw is rather thin (20 ft); however, this is a common thickness for one-cycle shoreline barrier reservoirs and is nearly the same as at Bell Creek.
2. No EOR processes have been implemented in the field although EOR is believed to be under consideration.

3. Few foreshore and shoreface intervals have been identified in examined reservoir cores.

Other Activities Related to Final Selection and Evaluation of Almond Formation/Patrick Draw Field

The process used to select the second reservoir for testing NIPER reservoir characterization methodology was presented to the BPO Project Manager, in January, 1990, and tentative approval for studying the Almond formation at Patrick Draw (WY) field was obtained. A trip was made to the USGS core-storage facility in Denver, and Upper Cretaceous Almond formation cores from Patrick Draw field were examined. The objective of this examination was to evaluate the quality of 34 slabbed cores from wells primarily in the Arch Unit of Patrick Draw field for the development of a generalized shoreline barrier model and comparison with the Muddy formation at Bell Creek (MT) field. It was concluded that the Arch Unit of Patrick Draw field was deposited in a mesotidal setting, whereas Bell Creek field is a microtidal shoreline barrier.

The office of Union Pacific Oil Resources, the operator of Patrick Draw field, was visited to examine the quality of geological and engineering data for the development of a generalized shoreline barrier model. It was learned that adequate core analyses and production-injection data are available from both the Arch and Monel Units. However, few well test data were collected in this field. A second meeting with the BPO Project Manager was arranged in March, 1990 for the purpose of sharing information about similarities and differences between Patrick Draw and Bell Creek fields based on initial findings.

An agreement for releasing reservoir data from Patrick Draw field was sent to Union Pacific Oil Resources, and a verbal agreement was obtained; however, no written confirmation has been received. A Union Pacific representative has indicated that transfer of information will probably occur during June, 1990.

Log and completion information about Patrick Draw field was received representing virtually all the data that were available from the USGS. Compilation into a computer data file of all the collected data was continued this quarter.

Data from Patrick Draw field are being entered into a spreadsheet data file as they are collected (appendix B). This organized, digitized form allows easy access to digitized data for any purpose including direct input of various parameters into computer mapping, log analysis, statistical analysis, graphics, and simulation programs. Direct transfer into a multi-use geological data base will be possible when the data base becomes available. Additional well, engineering, and production data will be added as they become available.

Currently the following parameters for 200 wells have been input into the spreadsheet data file:

(1) Location (section, township, range, footage from section lines);
(2) Elevation (ground level and Kelly bushing);
(3) Core information (slabbed or full, interval cored, photographs available/onhand, percent core recovered, quality of core);
(4) Total depth and tops of formations (Lance, Fox Hills, Lewis, Almond and Erickson);
(5) Logs run;
(6) Well status (gas/oil producer, gas/water injector, shutin , plugged and abandoned, temporarily abandoned, dry and abandoned, never drilled);
(7) Initial production (perforated zones, perforation density); and
(8) Oil gravity

Lithostratigraphic profiles and facies interpretation of two Almond formation cores from coreholes drilled behind outcrops on the eastern slope of the Rock Springs Uplift, about 40 miles apart, previously studied by Meyers (1977)[12] have been reexamined by NIPER geologists at the Occidental Petroleum Co. research facility in Tulsa, OK. The primary objective of the reexamination was to identity the sedimentologic criteria used by Meyers in the late 1970s for identification of facies in the Patrick Draw area and to compare the criteria used by NIPER geologists in the late 1980s in the Bell Creek area. Such "calibration" is necessary in comparative studies based on facies interpretations by geologists representing different schools but who must deal with assemblages of facies representing the same general environment of deposition but formed under different dynamic conditions.

Average grain size was measured on a foot-by-foot basis in a 300-ft interval of barrier/shoreline in Almond Core Hole No. 2. Descriptions of sedimentary/biogenic structures were also recorded. Alternative interpretations were suggested from those concluded by Meyers for some intervals. Additional work is being conducted to resolve these differences.

PALEOGEOGRAPHIC SETTING OF THE ALMOND FORMATION

The Almond formation, the upper interval within the Mesaverde formation, was deposited during a local regression in the overall transgression of the marine Lewis formation over the Mesaverde formation (Asquith, 1975).[13] It ranges in thickness from 250 to 750 ft and can be divided into lower and upper members. The lower Almond (100 to 600 ft thick) contains fresh water fauna of dinosaur, crocodile, turtle, and fish fossils and consists of small, lenticular channel sandstones; thin, finer-grained levee; overbank and floodplain sandstones, siltstones and mudstones; and carbonaceous shales and coal beds deposited in a fresh water, coastal swamp environment (Van Horn,1979).[14] The upper part of the lower Almond (125 to 250 ft thick) consists of a cyclic sequence of coals deposited in a fresh-water coastal-marsh environment and fossiliferous, slightly carbonaceous shales, mudstones, siltstones and thin sandstones deposited in a brackish-water, salt-marsh tidal flat, estuarine setting.

The upper Almond (100 to 400 ft thick) produces prolific amounts of oil and gas in the Greater Green River Basin and has been interpreted as a shoreline/barrier deposit.[6,11,14-17] It contains two distinct units consisting of fine-to medium-grained tidal channel/inlet deposits, and fine- to very fine-grained shallow marine deposits. In the Rock Springs/Patrick Draw area, barrier islands were deposited at the head of an embayment (Rock Springs Embayment) in an inter-deltaic area between the Red Desert delta[14, 17-19] to the north and an unnamed delta west of Craig in northwestern Colorado (fig. 2). Moderately high tides (greater than 3 ft) affected the development of the barrier islands and probably resulted from a focusing of tidal currents as they flowed westward and became constricted toward the head of the rock Springs embayment (Roehler, 1988).[11]

Depositional Environments

Tidal channel/inlet deposits are common in mesotidal barriers (tidal range 3 to 12 ft) (Hayes and Kana, 1976)[20] and are also present in the upper Almond formation in the Rock Springs area. Mesotidal channel/inlet sand bodies are associated with laterally migrating barrier-island tidal inlets (fig. 3). Inlet migration is the result of longshore drift which transports sediment in one dominant direction (shoreline parallel) resulting deposition on the updrift side and erosion on the downdrift side of each inlet. In the upper Almond, three sand bodies can be identified as components of the tidal inlet setting: (a) flood tidal delta, which forms on the landward (lagoonal) side of the inlet, interfingers with tidal flat and salt marsh deposits, and commonly contain oysters (*Crassostrea* sp.) at the base of the deposit; (b) tidal channel, characterized by scoured erosional bases, shell lags of abraded oyster valves and bimodal ebb and flood oriented cross-stratification; and (c) ebb tidal delta, form on the seaward side of tidal inlets, exhibit ebb oriented cross-strata where associated with tidal channel sandstones, and in a seaward direction, become massive and grade into marine sandstones.

The shallow marine sandstones were deposited on the seaward side of the barrier islands and represent outer shelf, subshoreface, shoreface and foreshore (beach) deposits (Van Horn, 1979).[14] Outer shelf deposits consist of commonly bioturbated shale and siltstones which grade upward into the subshoreface environments of interbedded sandstone, siltstone and shale deposited below daily wave base and commonly contain the trace fossils *Thalassinoides* and a miniature form of *Ophiomorpha* (Van Horn, 1979).[14] The shoreface sandstones were deposited below low tide and above effective wave base and commonly contain deposit feeding type burrows in the lower part and low-angle cross-stratification and abundant *Ophiomorpha* burrows in the upper part. In the Rock Springs/Patrick Draw area, the laterally extensive shallow marine sands are truncated by tidal inlet/channel deposits resulting in rapid lateral facies changes and complex reservoir unit geometries.

GEOLOGY OF PATRICK DRAW FIELD

The Almond formation is one of the most important hydrocarbon units in the Rocky Mountain region. This Upper Cretaceous (Maestrictian) shallow marine and coastal, coal-bearing sandstone has produced 100 million bbl of oil and 0.7 trillion cu ft of gas through 1986. (Keighin, et al., 1989).[21]

Hydrocarbon production from the Almond formation is located in the Greater Green River Basin, Sweetwater County, Wyoming and occurs on the eastern flank of the Rock Springs Uplift, northeastern flank of the Washakie Basin, and Wamsutter arch. The major fields producing oil from the Almond formation are Patrick Draw, Table Rock, and West Desert Springs. Desert Springs field produces gas. All of the fields are stratigraphic traps except Table Rock field, which is a structural trap.

Patrick Draw field is divided into two units, the northern Arch Unit and the southern Monel Unit (fig. 12). Table 6 presents reservoir properties and field data for Patrick Draw field. Attempts to waterflood the Arch Unit were unsuccessful due to the breakdown of incompetent coal beds within the reservoir. The Monell Unit, however, has been successfully waterflooded for 10 to 15 years, with current consideration of applying EOR methods to further enhance production.

Oil production in Patrick Draw field is from the upper 60 ft of the Almond formation which consists of two sands designated as the UA-6, the lower sand with an average thickness of 12 ft, and the UA-5, ranging in thickness from 0 to 30 ft (Weimer & Tillman, 1982).[23]

The UA-6 is oil productive in West Desert Springs field (fig. 4) and in the northern (Arch Unit) of Patrick Draw field (Weimer and Tillman, 1982).[22] The sandstone is gray, very fine-to fine-grained, calcareous and ranges from a wedge-edge to more than 25 ft thick. The UA-6 sandstone trends south-west to north-east and has been interpreted as tidal creek channels and tidal flat sands deposited landward (west) of a shoreline sand trend based on the erratic distribution of productive sandstone, the fine grain size, and the close association above and below with coal beds and lagoonal shale (Weimer and Tillman, 1982).[22] An alternative interpretation as a distributary channel has also been suggested.[23]

A second sandstone labeled UA-5 occurs near the top of the Almond formation and is the main oil productive sandstone at Patrick Draw. The UA-5 sandstone is interpreted as a prograding, shoreline sand that was deposited in a mesotidal regime (4 to 8 ft tidal range).[17] The UA-5 sandstone ranges in thickness from 0 to more than 30 ft within Patrick Draw. The porous and permeable UA-5 sandstone zone occurs over an area at least 20 miles long and 6 to 8 miles wide. The reservoir is sealed by the overlying marine Lewis Shale, by oyster-bearing (*Ostrea glabra*) coquina layers in the central part of the field, or by 5 to 10 ft of carbonaceous shale and impermeable sandstone.

The UA-5 interval has at least two distinct bars, and aresulting low permeability zone which runs mainly north-south and splits the Arch unit into two parts. Although the two bars are similar in lithologic character (Weimer, 1966),[18] they are nearly separate reservoirs with different oil-water contacts, one having a gas cap while the other does not. The permeability barrier represents a depositionally controlled heterogeneity consisting of oyster coquina layers, carbonaceous shale and impermeable sandstone which probably formed in a lagoonal setting.

The UA-5 can also be divided vertically into two main, mappable units in the Monell Unit (Champlin Interoffice correspondence). The upper part (A) is present over most of the west half of the Monel Unit, while the lower part underlies a consistent shale interval, and sometimes a coquina marker below the shale, in both the Arch and Monell Units. The best part of both the Arch and Monell Units is the lower UA-5 (B) sand, which normally has three to ten times the permeability of the upper UA-5 (A) sand.

The UA-5 (A) sand is also present in the Arch Unit and is thought to be correlative with the sand in the Monell Unit, but not hydraulically connected (IBID). This is supported by the fact that in the Arch Unit, the sand is wet and non-productive.

Tectonics of Patrick Draw Field and Adjacent Area

Patrick Draw oil field is located in the Greater Green River Basin, east of the Laramide-Aged Rock Springs Uplift, which divides the Green River sub-basin on the west from the Wasbakie sub-basin on the east. The Wamsutter Arch, which is an east-west structural nose on the east flank of the Rock Springs Uplift, separates the Great Divide sub-basin on the north from the Washakie sub-basin on the south. Thus, Patrick Draw field is structurally located on the eastern flank of the Rock Springs Uplift and on the southern limb of the east-west trending Wamsutter Arch dipping into the Washakie Basin (Richers, 1990 in press).[24]

Post-Laramide tectonism affected the present position of the Wamsutter arch and subsequently affected the position of oil and gas reservoirs exploited in the Patrick Draw area.[18] Vitrinite reflectance data,[25] recent thermal modeling, and general reconstruction of structural developments clearly indicate that the tectonic history in the Patrick Draw area played a decisive role in generation, original entrapment, and relocation of oil to the present position after the axis of the Wamsutter Arch migrated in the mid-Tertiary to the north and the Almond formation developed a dip of about 4 degrees in the Patrick Draw field area.

Post lower-Almond to early-upper Almond uplift was an early positive expression of the present Rock Springs Uplift-Wamsutter arch that caused truncation and westward thinning of lower Almond strata.[14] Structural downwarping west of Patrick Draw combined with the incipient Wamsutter Arch placed the Patrick Draw sandstone in a structurally high position with closure to the west, south, and north by the time the upper Almond strata were deposited.[14] The structurally high position promoted early hydrocarbon accumulation.[26] Much of the present-day Cretaceous section near Patrick Draw is currently in the oil window zone, actively generating hydrocarbons from the marine, organic-rich Lewis Shales.[24]

A number of east to northeast trending normal faults have been documented in the outcrop belt of Almond on the Rock Spring Uplift. Few of these faults, however, cut through Patrick Draw field (fig. 4). The movements on these faults is thought to be dominantly vertical. Several faults have characteristic normal fault dips that approach 45 degrees.[14] Richers, et al.[24,27] studied a relationship between geochemical anomalies observed in Patrick Draw area and distribution of faults and linaments (fig. 5). They concluded that fractures and faults are the prefered migration pathways of hydrocarbons leaking from the subsurface source beds and reservoirs to the surface.

Law, et al. (1986)[28] pointed out that vitrinite reflectance "anomalies" in the region of northeast trending faults cutting across Patrick Draw field indicate the possibility that hydrocarbons have migrated vertically along these faults from deeper basin pre-Almond source beds.

Weimer (pers. comm. in Van Horn, 1979)[14] indicated that the oil produced from the overlying Fox Hills formation as well as oil produced west of Patrick Draw migrated vertically from the Almond along east-west trending faults. The strong indications of lateral and vertical cross-formational flow through faults in Patrick Draw area should be confirmed by independent geochemical tools and isotopy.

Geochemistry of Fluids in Patrick Draw Field

Oil

Patrick Draw oil is moderately mature and paraffin based of 44.4° API gravity and density of 0.7977 g/cm^3 at 25° C (Richers, 1990).[24] The chemical composition of a Patrick Draw oil sample is shown in table 7. Whole oil chromatogram analysis indicates a preponderance of lighter n-paraffin components, a large amount the of isoprenoid pristane, and a composition supporting the premise that the oil is derived from terrigenous rather than marine organic matter.[24] Most geochemists believe that pristiane to phytane ratios greater than 3.0 characterize input from terrigenous material common to lacustrine, fluviatile, and deltaic environments, which fits the local geology of Patrick Draw. Vitrinite reflectance anomalies in the region discussed by Law, et al. (1986)[28] indicate the possibility of the hydrocarbons migrating vertically along northeast-trending faults from deeper terrigenous facies. This finding may imply geochemical heterogeneity of oils in different sections of Patrick Draw reservoir. Few data are available in the literature on lateral and vertical distribution of chemical, physical and isotopic properties of oil from the Patrick Draw field area.

Formation Water

Salinity and chemical composition of formation water in the Almond formation east of the Rock Springs Uplift varies significantly (Szpakiewicz and Collins, 1985).[29] In Patrick Draw field the downdip oil productive section of the Almond formation contains brackish waters with total dissolved solids (TDS) of 4 g/L and brines with a TDS of 70 g/L in the updip section (fig. 6). Chemical composition of the waters is highly variable. Chlorides, sulfates, or bicarbonates may locally predominate as the major anions in wells located about 1 mile apart.[29]

Geochemical inversion can be readily seen on a hydrochemical cross section (fig. 6). At depths of 3,000 to 4,000 ft in the updip mostly non-hydrocarbon-productive portion of Almond, highly saline waters (TDS = 50 to 70 g/L) overlay downdip formation waters associated with oil and gas accumulation having a salinity as low as 2 to 20 g/L. Mechanisms for forming these anomalies and heterogeneities can only be speculated at this time. Analyses of the stable isotope content of fluids could provide more definite answers. The problem is of more than academic nature because an anomalous inversion like that in Patrick Draw field seems to be a rule rather than exception in major petroliferous intermontane basins of the U.S. Rocky Mountains (Szpakiewicz and Collins 1985).[29] Little attention has been reported in the petroleum literature about the geochemical inversions in petroliferous basins which seem to be of widespread in geologically young basins.

A definite reverse gradient in water salinity existing in both the Arch and Monell Units of Patrick Draw field has been noticed by practitioners. Analyses of produced water also differ significantly in Monell and Arch Units. All Arch Unit wellhead samples contain large quantitites of sulfate ion (above 1 g/L) and bicarbonates predominate over chloride, whereas in Monell Unit water samples sulfates are virtually absent, and chloride, is a dominant anion. These facts strongly indicate that Almond waters in both units are not in hydraulic contact and belong to two different genetic systems.

A systematic study of chemical and isotopic characteristics of oils, waters, and gases in the geochemically heterogeneous Patrick Draw system could provide vital information for improvement of further development of the field and proper selection of EOR strategy.

Mineralogical Composition of the Almond Formation

Bulk mineral composition based on X-ray diffraction (XRD) of sandstones and shales of the upper portion of the Almond formation was presented by Keighin, Law, and Pollastro (1989).[21] Their results, reproduced here in table 8, indicate that sandstones in Patrick Draw reservoir tend to contain more carbonate minerals and less quartz than do upper Almond sandstones which are buried to greater depths east of Patrick Draw. Carbonates include calcite, dolomite, ankerite, and siderite. Keighin and others[21] noted that the amount of carbonate in the sandstone varies greatly on the scale of a few inches. In addition, ankerite is the most common carbonate cement in tightly cemented sandstones.

In a study of porosity occlusion in Upper Cretaceous sandstones from the Rocky Mountain Region (including the Almond formation), Jacka (1970)[31] noted that tops and bottoms of progradational barrier island sandstone bodies commonly exhibit greater concentrations of calcite cement than middle (foreshore beach and surfzone) intervals. He also noted that locally common concentrations of oyster shells in backshore beach or lagoonal sediments of Upper Cretaceous Rocky Mountain barriers may be so tightly calcite cemented that they could locally form seals to trap hydrocarbons. According to Jacka,[31] where oyster shells are not concentrated in lagoonal backshore (backbarrier) portions of barrier island sandbodies, porosity-occluding calcite cement is lacking. Jacka concluded that calcite cement in the Upper Cretaceous barrier island sandstones of the Rocky Mountains is a function of the abundance of calcite nuclei upon which the calcite crystals can grow. Calcite nuclei may be provided by oyster fragments, disagregated *Inoceramus* prisms, and planktonic and benthic foraminifera.

Table 8 indicates that total feldspar content of the Almond sandstones average 5%. Much detrital feldspar has been removed by dissolution and some has been replaced by carbonate minerals. Potassium feldspar (dominantly orthoclase) is more common in upper Almond sandstones at depths of less than 6,000 ft in contrast to plagioclase feldspar which is more common in the more deeply buried upper Almond sandstones.

Upper Almond sandstones contain between about 15 and 25 wt % clay minerals (table 1). Mean clay-mineral compositions in the less than 2μ (clay size) fraction show that kaolinite is the most abundant clay within the shallower reservoir sandstones. Kaolinite abundance decreases with increasing depth (table 9) and is rare to absent in reservoir sandstones below 9,000 ft.[21] Small amounts of chlorite were detected in Almond shales, but none was detected by Keighin et al.[21] in any sandstone samples. Illite dominates the clay size fraction below 9,000 ft and includes discrete illite and interstratified illite/smectite. Illite/smectite is of the ordered variety and contains less than 25% expanded layers.[21] Little smectite is found in either the upper Almond formation sandstones or in the shales. These characteristics of the clay composition indicated to Keighin, et al.[21] that even the shallowest upper Almond formation reservoir rocks, now at depth of approximately 4,500 ft may have been buried to depths where the temperature exceeded 212° F, or may have experienced a heating event.

Four additional samples from Patrick Draw field have been analyzed by X-ray diffraction during the course of our studies. The results (table 10) tend to support the results of Keighin, et al.[21] in that quartz is the dominant mineral except in sample 45-14-3 (50 ft), which was from an oyster rubble bed. K-feldspar is dominant over plagioclase, kaolinite is the dominant clay mineral, and illite and mixed-layer illite/smectite are present.

Excluding the sample from an oyster bed, calcite comprises less than 5 wt % of the samples; however, combined dolomite and ferroan dolomite comprise up to 25% in one sample. Total carbonate content ranges from 12 to 93 wt % of the samples and is dominated by ferroan dolomite. The amount of dolomite from samples in table 10 is much greater than that indicated by Keighin, et al.[21] (table 9). The greatest amount of dolomite plus ankerite (ferroan dolomite) reported by Keighin, et al. was only 12%, although the greatest amount of total carbonate was 20 wt % - which is in line with most of the values in the Patrick Draw samples (table 10).

Petrographic analysis of Almond formation outcrop thin sections by Pryor[30] indicate a very similar mineralogical composition as compared to analyses by Keighin, et al.[21] Point count analysis by Pryor indicates an immature chert arenite composition. Twenty-nine Almond reservoir samples examined by Thomas (1978)[32] were classified as quartz arenite, however, chert and other quartzose rock fragments were plotted on the same pole of a sandstone composition classification diagram. If corrections for rock fragments were taken into account, the samples from Thomas[32] would plot in the sublitharenite to chert arenite range of the classification scheme of Folk (1968).[33] Detrital matrix contributed 16.5% of the rock volume while rock fragments contributed 25% of the total rock composition in the samples from Pryor.[30] A generic classification of the rock fragments include the following: shale, 0.5%; siltstone, 1.5%, chert,19.5%; and polycrystalline quartz, 3.5%. Van Horn (1979)[14] noted that chert decreases volumetrically with respect to feldspar in an up-section direction within the upper Almond formation. He also concluded that the abundance of pelitic rock fragments in upper Almond sandstones places the feldspar and lithic (rock fragment) content nearly equal. The finer grained sandstones (with an abundance of pelitic rock fragments) fall into the litharenite to sublitharenite category, while the coarser sandstones (which are relatively deficient in the pelitic rock fragments) fall into the arkosic to subarkosic category. If, however, the pelitic rock fragments are fecal pellets (which is not unlikely) then the coarser upper Almond sandstones could all be classified as arkoses to subarkosic arenites by the system of Folk.[33] Heavy mineral content was less than 0.8% for all Mesaverde Group sandstones analyzed. Garnet and zircon comprised 94% of the heavy mineral abundance in an Almond sample[30] indicating crystalline schists, gneiss, and acid igneous source rocks.

Texture of Almond Reservoir Sandstones

Lower Almond formation (fluvial and freshwater coastal marsh; Van Horn, 1979[14]) reservoir rocks consist of pods of poorly sorted, very fine-grained, silty, agrillaceous (illitic) sandstone. Lower Almond sandstones would be moderately-well to well-sorted if it were not for the abundance of silt and clay matrix.[14] In contrast, upper Almond reservoirs consist predominantly of medium-grained sandstones. These coastal and barrier sandbodies[6,18,34] consist of well sorted, linear belts containing much smaller percentages of authigenic clay, which is dominantly kaolinite.[32] The major carbonate mineral in upper Almond reservoirs is calcite or dolomite, whereas it is frequently siderite in the lower Almond. Carbonate cement and compacted clay-rich rock fragments (fecal pellets?) significantly reduce porosity in most upper Almond sandstones[14] and thinner, finer-grained units are more tightly cemented by authigenic carbonate than are thicker upper Almond sandstone units. Fine-grained and medium-grained upper Almond sandstones have similar fabrics dominated by point contacts and include many floating grains, suggesting that early cementation prevented later compaction.[14]

Rock Structure and Anisotropy

The CT scanner is being used to generate vertical density attenuation profiles for cores from Patrick Draw field. The developed software will be used to calculate the fractal dimension from CT profiles.

Three slabbed rock samples from Patrick Draw cores well 49-1-3, 4,522 ft (fig. 7), 4,531 ft (fig. 8), and well 7-18-1, 4,957 ft (fig. 9) were CT-scanned perpendicular to bedding to evaluate the extent of CT density variation within facies having different reservoir quality. Sample 7-18-1, 4,957 ft has the best reservoir quality (greatest apparent porosity based on visual scan) and has a CT density that varies from 600 to 700 H.U. This sample is a porous, cross-laminated fine-grained sandstone with a few partly cemented thin laminae. The intermediate reservoir quality sample (49-1-3, 4,522 ft), which is a thinly laminated silty sandstone with more visible lamination has CT density variation from 650 to 750 H.U. The sample with the poorest reservoir quality (49-1-3, 4,531 ft) comprises interlaminated silty very-fine sandstone and silty shale. It has a CT density variation of 750-850 H.U. Note that CT density increases with generally decreasing reservoir quality and that even the "better" layers (lower CT values) in successively poorer reservoir quality rock do not seem to overlap.

This type of CT density variation reflects a high degree of vertical anisotropy related to interlayering of lithologies within the core samples. The CT density variation in the best reservoir quality sample is determined by relatively small amounts of clay cementation based on thin section analysis.

A sample of black, coaly siltstone and shale (well 78-14-6, 4,344 ft) was also scanned (figure 10) and shows CT density increasing from 0 to about 450 H.U. as one proceeds away from the thin pure coal layers into dark-colored siltstone and shale. This transitional behavior, shown on the scan profile in figure 10, reflects several coal-rich laminae that can be distinguished from the surrounding silty shale and indicates a transitional or alternating environment.

Diagenesis of Almond Reservoir Rocks

The diagenetic history of the Almond marine reservoirs is complex. Keighin, Law, and Pollastro (1989)[21] distinguished nine stages in their evaluation (fig. 11). Quartz overgrowths on detrital quartz grains were found in all samples they examined. Most quartz overgrowths precipitated early in the paragenetic sequence, however, some was found to reduce porosity within secondary pores. Five to 15% of the primary porosity in upper Almond formation sandstones has been filled by silica cement. The diagenetic sequence for upper Almond sandstones proposed by Thomas[32] is somewhat more simplified; however, it is in very close agreement with the scheme presented by Keighin, et al.[21]

Most of the porosity in the Almond sandstones at Patrick Draw field has been created by the dissolution of mineral grains and cement.[21] Most intergranular porosity is due to the dissolution of ferroan calcite cement, while most intragranular and moldic porosity was formed by dissolution of feldspars, chert, and shale rock fragments. Because the reservoir sandstones generally contain a significant amount of easily decomposed rock fragments (such as chert and shale) the rock fragments make the reservoir rock sensitive to compaction and subsequent decrease in porosity and permeability. The rock fragments are commonly altered or leached to variable degrees resulting in creation of abundant microporosity that contributes little to permeability.

In contrast, some of the shallow (4,500 to 5,800 ft) reservoir sandstones remain tightly cemented by what Keighin, et al.[20] called ankerite, which is ferroan dolomite (table 10, sample 7-18-1, 45 ft). Ferroan dolomite is common in the shallower Almond formation reservoir sandstones where it replaces calcite and quartz cement, and also is found as syntaxial overgrowths on dolomite.

Clay minerals play an important role in the development of reservoir quality. Partial dissolution and replacement of rock fragments by clays, as already stated, created microporosity but did not significantly contribute to permeability. The habit and distribution of clays within the pore system indicate that the reservoir should be sensitive to migration of fines as described by Priisholm, et al. (1987).[35] Cementation and replacement of detrital chert, quartz grains, shale rock fragments, and clay matrix by kaolinite is extensive in the Patrick Draw area.[21] Illite cementation is a major mid- to late-stage event in the Almond, particularly in the deeper (>8,000 ft) reservoir sandstones. Illite replacement of rock fragments was reported in Almond sandstones from 4,500 to 12,000 ft.[21] Illite with "flame-like" and acicular habits is also present within secondary pores.

The development of authigenic illite in Almond reservoir rocks is thought to be partly due to the conversion of smectite to illite (Pollastro, 1985),[36] and partly to earlier leaching of K-feldspars.

It may be expected that outcrop samples from analogous sandstones may have a somewhat different diagenetic sequence which may at least in part be controlled by their more complicated tectonic history. Jacka (1970)[31] suggested that as a result of uplift into the vadose zone iron hydroxide may be deposited as coatings or as "ironstone" concretions. Also, calichefication of calcite-cemented horizons may occur upon uplift and exposure to vadose conditions. Distinguishing caliche created by outcrop weathering from that produced by early re-emergence of calcite-cemented reservoir barrier sandstones will require careful stratigraphic and petrographic studies.

Porosity

A plot of porosity versus depth for sandstone core samples from the Almond formation[21] indicates the expected relationship of decreasing porosity with increasing depth. There is, however, a much greater scatter for data in the lower porosity rocks (<8%) that generally occur below about 9,000 ft. The shallower sandstones are conventional reservoirs with porosities as great at 22% (Patrick Draw field), while the deeper sandstones have porosities that range from 3.5 to 8% and are generally unconventional (tight) reservoirs.

Based on vitrinite reflectance, there is also a generic relationship between decreasing porosity with increasing thermal maturity.[21] Another conclusion about the development of porosity in the Almond formation is that Patrick Draw area fields had experienced a heating event. Law, et al. (1986)[28] concluded that the unusually high levels of thermal maturity in the field and the area around Patrick Draw were due to upward migration of hot fluids along faults and fractures. Such conditions may enhance or decrease porosity depending on the composition of the fluids and the nature of their interaction with the reservoir rocks.

Permeability and Pore Throat Sizes

Porosity versus permeability for Almond formation sandstones show two distinct permeability regions. The more porous sandstones (>10% ø, >1 md) show a well-defined trend of increasing permeability with increasing porosity.[21] The data from lower porosity/lower permeability (generally less than 1 md) rocks display greater scatter and a much more poorly defined trend. Based on mercury injection-capillary pressure data[21] and thin section examinations, the pore throats in Almond formation sandstones are frequently smaller than 1 micron in diameter. Effective pore throat size (where mercury begins to enter the pore throats) for samples from Patrick Draw field is generally between 10 and 15 μ, whereas effective throat size for deeper Almond sandstones is much more variable and generally smaller. The variations in pore throat size for deeper samples is controlled by grain size, amount of carbonate cement and presence or absence of microfractures.

GEOLOGICAL AND PETROPHYSICAL PROPERTIES OF RESERVOIR SANDSTONES OF UPPER ALMOND FORMATION - PATRICK DRAW FIELD, WY

The distribution pattern and continuity of sandstones and other stratigraphic units of the upper Almond formation in Patrick Draw field were investigated from a dip-oriented stratigraphic section in the north central part of the field (see fig. 12 for location). The stratigraphic section was (fig. 13) constructed from available induction and Sp logs, but other logs, such as sonic and density, were also studied when available. Preliminary lithological description of cores performed by NIPER geologists and earlier workers were available from a few wells along this section for calibration of log signatures with the dominant geological features.

Stratigraphic Units

The following stratigraphic units are important from considerations of oil and gas accumulations and could be differentated on the stratigraphic section (fig. 13).

1. The lowermost unit consists of a cyclic sequence of shales, sandstones, and coals each of which has a typical log signature. Particularly, the numerous coal beds are distinguishable by their sharp resistivity 'kicks' on induction log and very high transit time 'kicks' on the sonic logs. Three distinct cycles in this sequence were previously distinguished (McCubbin and Brady, 1969), [34] out of which cycle II is important because it contains the oil producing UA-6 sandstone. The UA-6 sandstone is either absent or is very thin (4 ft or less) in figure 13 and is not always easily distinguishable on logs from the few other thin sandstone beds in this area. The UA-6 sand has good development slightly north of the section such as at well 64, section 11.

2. The lowermost of the shale units in this sequence can be easily distinguished and correlated on electric logs across the entire stratigraphic section. This unit has been called the 'marker shale' by Weimer (McCubbin and Brady, 1969).[34]

3. Above the 'marker shale' and separated from it by another cycle of sandstones, shales and coals in most parts of the stratigraphic section is the producing UA-5 sandstone, which has been interpreted to be a shoreline/barrier deposit. The UA-5 sandstone is the principal reservoir in Patrick Draw field and is easily distinguishable on electric logs. It may be seen in figure 13 that

the UA-5 sandstone deposit is composed of two distinct 'bars' (the so-called 'western' and the 'eastern' bar) separated from each other by a zone where the sandstone is absent.

4. All along the 'western bar' and in the western part of "eastern bar' an oyster bearing layer of shales and sandstones overlie the UA-5 sandstone. This oyster-bearing layer is thickest where it fills the low between the two bars (about 30 ft) and is easily distinguishable on electric logs by its characteristic sharp response.

5. Directly overlying the Almond formation are the marine 'Lewis' shales. The contact between the Lewis and the oyster layer is easily distinguishable and correlatable on all the logs in the study area.

Petrophysical and Reservoir Properties of UA-5 Sandstone

The oil and gas accumulation in UA-5 sandstone at Patrick Draw is the result of a stratigraphic trap formed by updip pinchout of the bar westward into impermeable lithologies. Generally the UA-5 sandstone is well sorted, fine-grained and it has uniform texture and composition with a minor degree of stratification. X-ray diffraction and clay/mineral analysis (tables 8-10) show that the UA-5 sandstone consists of (in decreasing order) quartz, carbonate minerals, clay minerals, and feldspar. Substantial amounts of authigenic clays are also present as pore-lining and pore-filling material.

The distribution of porosity and permeability along the entire thickness of the UA-5 sandstone can be studied from the type logs such as the ones from wells 10-A and 102 (figs. 14 and 15) located close to the stratigraphic section (see fig. 12 for location). Typically the average porosity is around 20% which is sometimes drastically reduced at the top of the sand, due to dolomite cementation (well 102, fig. 15). If the upper cemented zone is excluded, the amount of cement in the remaining sandbody is small. The uniform distribution in porosity is sometimes also disturbed by the presence of bioturbated zone (a and 'shell bed' which drastically reduce porosity (fig.14). The vertical distribution of permeability follow the same trend as the porosity but its variation is more drastic and in the two wells (figs. 14 and 15) permeability values range between 0 and 150 md.

The distribution of grain sizes in the UA-5 sandstone, on which the petrophysical properties depend to a large extent, is usually fairly uniform in the vertical direction excepting that in many of the wells the sand is coarsest at or very near the base of the sandstone (McCubbin and Brady, 1969).[34] This increase in the grain sizes at the base of the sandstone is reflected by high permeability values in well 102 (fig. 15) at a depth of around 4,895 to 4,898 ft. From a few feet above the base, where the sandstone is finest, the grain size generally increases upward, suggesting deposition in progressively shoaling water. Laterally, the UA-5 sandstone becomes finer and less well sorted (McCubbin and Brady, 1969)[34] to the east of the 'eastern bar' where the sandstone grades laterally into marine shales in that direction. Presumably the petrophysical property will also continue to deteriorate in that direction.

PRELIMINARY ENGINEERING DATA ANALYSIS OF THE PATRICK DRAW FIELD

Reservoir History

Patrick Draw field is located in townships 18 and 19 north, ranges 98 and 99 west, Sweetwater County, in Southwestern Wyoming. The field was discovered on April 11, 1959, with the completion of the discovery well, El Paso Natural Gas Co., Patrick Draw Unit 1. Initial production rate for this well was 638 BOPD. Oil and gas were found at a depth of about 4,600 ft in the upper Cretaceous Almond Sandstone (Mesaverde Group). The reservoir drive mechanism for primary production was mainly solution-gas, and no active water encroachment was reported. Gas was generally not produced but reinjected through two injection wells for reservoir pressure maintenance. Waterflooding was initiated in 1963 and 1966 for the Monell and Arch Units, respectively. A full-scale waterflood was implemented on 80 acres with a 5-spot pattern along with water injection at the gas-oil contact for improving injectivities. About 239 wells have been drilled, and about 128 of these have been water injection wells. Both initial reservoir and saturation pressures were 1,790 psig. Average porosity and permeability are 20% and 26 md, respectively. Average net pay is 20 ft. A comparison of reservoir properties between Patrick Draw and Unit 'A' Bell Creek field is shown in table 6. Lower waterflood recovery from Patrick Draw field indicates higher degree of reservoir heterogeneities as compared to Bell Creek field.

Reserves

The total original oil-in-place (OOIP) for both the Arch and Monell units was estimated between 200 and 250 MMSTB from volumetrics, and between 140 and 150 MMSTB from material balance calculations. A total of approximately 78.5 MMSTB (35% OOIP) has been produced through primary and secondary operations. Table 6 also shows the primary and secondary reserves for Arch and Monell Units. These data indicate that the Monell Unit has a higher recovery efficiency than the Arch Unit. As of July 1983, the daily oil production for the Arch and Monell Units was 180 and 1,300 BOPD, respectively.

Well Completion Data

Average well diameter is 8 inches. Most wells were completed with 5 1/2-inch casing and 2-inch tubing and were perforated at four (most frequently used) or two shots per foot. All wells were stimulated by using acidization and hydraulic fracturing.

Core Analyses

From studies reported by McCubbin and Brady (1969)[34], the average permeability of the UA-5 sandstone ranges between 10.4 and 54.4 md. Routine core analyses results conducted at NIPER on core samples from well 120, Arch Unit shows that the average vertical permeability measured on full diameter core (10 md) is about half as much as horizontal permeability (18.6 md) of plugs samples using air. Similar conclusions were reached when a 6-inch-long core from higher energy facies of well 7-18-1, Arch Unit was CT scanned (fig. 9). The density profile along the long axis of the core indicates that CT density fluctuation due to lamination in the core is not very significant. The average grain density of core plugs from this well is 2.65 g/cm^3.

Table 11 shows results of permeability tests conducted on 154 samples from 26 wells in Patrick Draw field (Baptist, White, and Land, 1964).[37] Results indicate moderate formation sensitivity to fresh water flow. The reduction of permeability to fresh water is attributed to fineS migration resulting from illite and kaolinite presence in Patrick Draw field.

An imbibition and drainage oil-water relative permeability analysis conducted on a core sample from well 1 (Core Laboratories Scale 309-81274) is shown in figure 16. The residual water and oil saturations are between 51 and 58% and 18 and 20% respectively. The water relative permeability at residual oil saturation is 3.5%. The preservation and core preparation is not known at this time; however, the fluid flow performance of the core indicates that the wetting preference is strongly water-wet.

Typical mercury injection measurements performed on five core samples from Arch Unit of Patrick Draw field are shown in figure 17. More than half of the pore throat diameters of productive sandstone cores are between 2 and 20 microns, which is in agreement with results presented by Keighin, Law, and Pollastro (1989).[21]

A correlation between porosity and depth of burial showing decreasing porosity with increasing depth, has been reported by Keighin, Law, and Pollastro (1989)[21] Porosity reduction of as much as 20% with increase in the net confining pressure up to 2,750 psi has also been reported. Pore volume compressibility associated with the porosity reduction is between $4\text{-}8 \times 10^{-6}$ psi.

REFERENCES

1. Reinson, G. E. Barrier-Island and Associated Strand-Plain Systems, in Walker, R. G., Facied Models, Second Edition, Geoscience Canada. Reprint Series 1, 1984, p. 119-140. First edition published in 1979.

2. Szpakiewicz, M., R. Tillman, S. Jackson, and G. deVerges. Sedimentologic Interpretation of Barrier Island and Related Deposits in the Bell Creek Cores, Montana and Analogous Outcrops Near New Haven, Wyoming. NIPER Open File of Field Investigations, 1988. Available from the Authors.

3. Szpakiewicz, M., R. Schatzinger, M. Honarpour, M. Tham, and R. Tillman. Geological and Engineering Evaluation of Barrier Island and Valley-Fill Lithotypes in Muddy Formation, Bell Creek Field, Montana, in Coalson, E. B., ed., Petrogenesis and Petrophysics of Selected Sandstone Reservoirs of the Rocky Mountain Region. The Rocky Mountain Association of Geologists, Denver, Colorado, 1989, p. 159-182.

4. Schatzinger, R. A., M. Szpakiewicz, and B. Sharma. Applicable Correlations and Overall Characteristics of Barrier Island Deposystems. Department of Energy Report No. NIPER-427, August, 1989.

5. Campbell, C. V. Model for Beach Shoreline in Gallup Sandstone (Upper Cretaceous) of Northwestern New Mexico. New Mexico Bureau of mines and Mineral Resources, Circular 164, 1979.

6. Flores, R. M. Barrier and Back-Barrier Environments of Depositon of the Upper cretaceous Almond Formation, Rock Springs Uplift, Wyoming. The Mountain Geologist, v. 25, 1978, p. 57-65.

7. Galloway, W. A. Reservoir facies Architecture of Microtidal Barrier System. AAPG Bull., v. 70, 1986, p. 787-808.

8. Dixon, J. Mobil Oil Co., Dallas, TX. Personal communication.

9. Tillman, R. W. The Tocito and Gallup Sandstones, New Mexico, A Comparison, in R. W. Tillman, and R. G. Walker, eds., shelf Sands and Sandstone Reservoirs. SEPM Short Course No. 13, 1985, p. 402-464.

10. Wheeler, D. M., E. R. Gustason, and M. J. Furst. The Distribution of Reservoir Sandstone in the Lower Cretaceous Muddy Sandstone, Hilight Field, Powder River Basin, Wyoming. In: Giant Oil and Gas Fields, A Core Workshop. SEPM Core Workshop No. 12, 1988, p. 179.

11. Roehler, H. W. The Pintail Coal Bed and Barrier Bar G - A Model for Coal of Barrier Bar-Lagoon Origin, Upper Cretaceous Almond Formation, Rock Springs Coal Field, Wyoming. USGS Prof. Paper 1398, 1988.

12. Meyers, W. C. Environmental Analysis fo Almond Formation (Upper cretaceous) From the Rock Springs Uplift, Wyoming. Ph. D. Dissertation, University of Tulsa, 1977.

13. Asquith, D. O. Petroleum Potential of Deeper Lewis and Mesaverde Sandstones in the Red Desert, Washakie and Sand Wash Basins, Wyoming and Colorado. Rocky Mountain Association of Geologists Symposium, 1975, p.159-162.

14. Van Horn, M. D. Stratigraphy of the Almond Formation, East-Central Flank of the Rock Springs Uplift, Sweetwater County, Wyoming: A Mesotidal Shoreline Model for the Late Cretaceous. M.S. Thesis, Colorado School of Mines, 1979, 150 p.

15. Hale, L. A. Stratigraphy of the Upper Cretaceous Montana Group in the Rock Springs Uplift, Sweetwater County, Wyoming. Wyo. Geol. Assoc. Guidebook, 5th Ann. Field Conf., 1950, p. 49-58.

16. Weimer, R. J. Upper Cretaceous Stratigraphy, Rocky Mountain Area. AAPG Bull., v. 44, 1960, p. 1-20.

17. Jacka, A. D. Sediment Economics of Upper Cretaceous Sandstones Rocky Mountain Region. Wyo. Geol. Assoc., 22nd Ann. Field Conf. Guidebook, 1970a, p. 187-219.

18. Weimer, R. J. Time-Stratigraphic Analysis and Petroleum Accumulations, Patric Draw Field, Sweetwater County, Wyoming. AAPG Bull., v. 50, 1966, p. 2,150-2,175.

19. Asquith, D. O. Depositional Topography and Major Environments, Late Cretaceous, Wyoming. AAPG Bull., v. 54, 1970, p. 1,184-1,224..

20. Hayes, M. O., and T. W. Kana. Terrigenous Clastic Depositional Environments. Coastal Research Division, Department of Geology, University of South Carolina, Technical Report 11-CRD, 1976, pt. 1, 131 p., pt. 2, 185 p.

21. Keighin, C. W., B. E. Law, and R. M. Pollastro. Petrology and Reservoir Characteristics of the Almond Formation, Greater Green River Basin, Wyoming. In Coalson, E. B., and others, eds., Petrogenesis and Petrophysics of Selected Sandstone Reservoirs of the Rocky Mountain Region. The Rocky Mountain Association of Geologists, 1989, p. 281-298.

22. Weimer, R. J., and R. W. Tillman. Sandstone Reservoirs. SPE 10009, Pres. at the International Petroleum Exhibition and Technical Symposium of the SPE, Bejing, China, 1982, p. 1-5.

23. Keyes, S. Union Pacific Resources Co. Personal communication.

24. Richers, D. M. Patrick Draw Oil Field. Preprint, To Be Published in: AAPG Treatise on Petroleum Geology, 1990.

25. Law, B. Relationships of Source-Rock, Thermal Maturity, and Overpressuring to Gas Generation and Occurrences in Low-Permeability Upper Cretaceous and Lower Tertiary Rocks, Greater Green IIRiver Basin, Wyoming, Colorado, and Utah. In Woodward, J., F. Meissner, and J. Clayton, eds., Hydrocarbon Source Rocks of the Greater Rocky Mountain Region. Rocky Mountain Association of Geologists, 1984, 557 p.

26. Weimer, R. J. Rates of Deltaic Sedimentation and Intrabasin Deformation, Upper Cretaceous of Rocky Mountain Region. in Morgan, J. P., ed., Deltaic Sedimentation Modern and Ancient. Soc. Econ. Paleon. and Mineral., Spec. Pub. 15, 1970, p. 270-292.

27. Richers, D. M., J. R. Reed, K. C Horstman, G. D. Michels, R. N. Baker, L. Lundell, and W. Marrs. Landsat and Geochemical Study of Patrick Draw Oil Field, Sweetwater County, Wyoming. AAPG. Bull., v. 66, 1982, p. 903-922.

28. Law, B. E., M. R. Lickus, and M. J. Pawlewicz. Fluid Migration Pathways-Evidence from Thermal Maturity Mapping in Southwestern Wyoming. USGS Circular 0974, 1986, p. 35.

29. Szpakiewicz, M., and A. G. Collins. Hydrochemical Study of the Upper Cretaceous and Lower Tertiary Formations in the Uinta, Piceance and Greater Green River Basins; Implications for Oil and Gas Related Problems. Topical Report NIPER-95, 1985, 70 p.

30. Pryor, W. A. Petrography of Mesaverde Sandstones in Wyoming. Wyoming Geol. Asoc. 16th Ann. Field Conf. Guidebook, 1961, p. 34-46.

31. Jacka, A. D. Principles of Cementation and Porosity-Occlusion in Upper Cretaceous Sandstones, Rocky Mountain Region. Wyoming Geol. Assoc. 22nd Ann. Field Conf. Guidebook, 1970b, p. 265-285.

32. Thomas, J. B. Diagenetic Sequences in Low-Permeability Argillaceous Sandstones. Jour. Geol. Soc. London. v. 135, 1978, p. 93-99.

33. Folk, R. L. Petrology of Sedimentary Rocks. Hemphills, Austin, Texas, 1968, p. 124.

34. McCubbin, D. G., and M. J. Brady. Depositional Environment of the Almond Reservoirs, Patrick Draw Field, Wyoming. The Mountain Geologist, v. 6, 1969, p. 3-26.

35. Priisholm, A., B. L. Nielson, and O. Haslund. Fines Migration, Blocking, and Clay Swelling of Potential Geothermal Sandstone Reservoirs, Denmark. SPE Formation Evaluation, v. 2, 1987, p. 168-178.

36. Pollastro, R. M. Mineralogical and Morphological Evidence for the Formation of Illite at the Expense of Illite/Smectite. Clays and Clay Minerals, v. 33, 1985, p. 265-274.

37. Baptist, O.C., E.J. White, and C. S. Land. Laboratory Predictions of Water Sensitivity Compared with Field Observations of Well Damage-Patrick Draw, Wyoming. SPE Paper 839, 1964, 6 p.

38. Sneider, R. M., F. H. Richardson, D. D. Paynter, R. E. eddy, and I. A. Wyant. Predicting Reservoir Rock Geometry and Continuity in Pennsylvanian Reservoirs, Elk City Field, Oklahoma. Jour. of Petroleum Technology, 1977, pp. 851-866.

39. Tomkins, J. Q. Bisti Oil Field, San Juan County, New Mexico. Amer. Assoc. Petrol. Geol. Bull., v. 41, 1957, pp. 906-922.

40. McNeal, R. P. Hydrodynamic Entrapment of Oll and Gas in Bisti Field, San Juan County, New Mexico. Amer. Assoc. Petrol. Geol. Bull., v.45, 1961, pp. 315-329.

TABLE 1. - Oil fields producing from shoreline barrier deposit. Initial candidates for comparative study and generalization of reservoir models

Atkinson	Texas
Bisti	New Mexico
Brent (North Viking Graben)	North Sea
Desert Springs	Wyoming
Echo Springs	Wyoming
Elk City	Oklahoma
Hilight	Wyoming
Jackson-Yegua	S. Texas
Livingston	Louisiana
Lockhard	Louisiana
Milbur	Texas
North Marklam-North Bay City	Texas
Patrick Draw	Wyoming
Pollard	Alabama
Sun Ranch	Wyoming
South Carlton	Alabama
Table Rock	Wyoming
West Ranch	Texas

TABLE 2. - Top five shoreline barrier reservoir candidates for comparison with Bell Creek field

Field/State	Basin	Formation	Depth, ft	Operator	Cores available	References
1. Patrick Draw, WY	Green River	Almond	4,000-5,000	Union Pacific & Texaco	USGS, Denver	[11]Roehler, 1988 [21]Keighin et al., 1989
2. Hilight, WY (Springer Ranch Member)	Powder River	Muddy	2,200-9,800	Inexco Oil Co.	RPI International Inc.	[10]Wheeler, et.al. 1988
3. West Ranch, TX						
Greta Reservoir	Gulf Coast	Frio	5,100	Mobil	Mobil, Dallas	[7]Galloway, 1986
Glasscock Reservoir	Gulf Coast	Frio	5,500	Mobil	Mobil, Dallas	[7]Galloway, 1986
41-A Reservoir	Gulf Coast	Frio	5,700	Mobil	Mobil, Dallas	[7]Galloway, 1986
4. Elk City, OK	Anadarko	Penn SS	9,400	Shell	Unknown	[38]Sneider et al., 1977
5. Bisti, NM	San Juan	Gallup	4,920	Shell Chevron Texaco & an Independent	Unknown	[39]Tomkins, 1957 [40]McNeal, 1961

TABLE 3. Comparison of depositional setting, some rock, and some fluid properties for Bell Creek field Unit "A", and the top five candidates for a comparative study

Field/reservoir	Reported environments	Avg net pay, ft	Avg porosity, %	Avg permeability, md	Water saturation, %	Estimated OOIP, MM bbl	Oil gravity Avg, °API
1. Patrick Draw	Barrier Island and Inlet Fill	14	19	50	–	200-250	42
2. West Ranch							
Greta	Aggrading Barrier Island	35	31	1,000+	33	223	24
Glasscock	Transgressive Barrier Island	20	29	540	45	127	31
41-A	Progradation Barrier Island	31	30	900	28	149	32
3. Elk City	Associated Delta and Barrier Bar	40	20	375	–	100	–
4. Bisti	Barrier Bar System	10	15	28	25	150	39
5. Hilight (Springer Ranch Member)	Progradational Barrier Island/spit and tidal inlet deposits	3 to 33 ft	–	–	–	–	40+
6. Bell Creek	Barrier Island and Valley Fill	23	28.5	2,250	26	127	32

TABLE 4. -Shoreline barrier outcrops considered for generalization of reservoir models

Almond Sandstone	Wyoming
Cliff House Sandstone	New Mexico
Eagle Sandstone	Montana
Ferron Sandstone	Utah
Fox Hills	Wyoming
Gallup Sandstone	New Mexico
Highway Roadcut	Kentucky
Holy Cross Mts. Miocene SS	Poland
Lower Jurassic	South England
Muddy Sandstones	Wyoming
Pictured Cliff Sandstone	New Mexico
Point Lookout Sandstone	New Mexico
Tocito Sandstone	New Mexico
Viking Sandstone	Alberta, CA

TABLE 5. - Modern shoreline barriers considered for generalization of reservoir models

Atlantic Coast, USA	
The Outer Banks	North Carolina
Wassaw Island	Georgia
Baltic Sea Coast	
Hel Pennisu	Poland
VistulaBarrier Bar	Poland
Kuronsky Barrier Bar	USSR
Gulf of Mexico	
Galveston Island	Texas
Padre/Mustang Islands	Texas
North Bunces Key	Florida
North Sea Coast	
East Frisian Islands	Germany
Terschelling Island	Netherlands

TABLE 6. - Reservoir data and history for Patrick Draw field

	Patrick Draw	Bell Creek 'A'
Discovered	1959	1967
OOIP - Arch unit, MM STB	97.6	
OOIP-Monell unit, MM STB	112.5	
Total OOIP, MM STB	220-250	127
Primary	Solution Gas	Solution Gas
Arch, %	17.7	--
Monell, %	20.0	--
Bell Creek, %	--	17.3
Secondary	Five-spot waterflood	Linedrive WF
Arch, %	12	--
Monell	15	--
Bell Creek, %	--	36.7
Total recovery, MM STB	78.5 (35% OOIP)	68.6 (54%)
ROS after waterflood, % PV	39	35
Sor, % PV	19.5	30
Oil viscosity,cP	0.52	2.76
Porosity, %	19.8 (12-22)	28.5
Permeability, md	35.9 (5-200)	915 (50-7000)
Interstitial water saturation, %	30-50	20-35
Gas-oil contact, ft	+2525	+2475
Water-oil contact, ft	+1450	+1635
Oil gravity, °API	42	32.5
Initial oil formation volume factor vol/vol	0.52	0.76
Temperature, °F	121	110
Initial pressure, psi	1790 @ +2000'	1204 @ -800'
Saturation pressure, psi	1790 @ +2000'	1204 @ -800'
Initial solution GOR, SCF/bbl	450	200
Net pay, ft	20	22.9
Field size, acres	16,540	7,219
Length - width, miles	9-3	5-2
Depth, ft	5100	4500
DIP, degrees	4	1
HC Porosity	0.13	0.2
Dominent clay	Kaolinite/Illite-Smectite	Kaolinite

TABLE 7. - Chemical composition of a Patrick Draw oil sample. After Richers[24]

Oil Weight	Normal C9+	Saturates	Aromatics	Resin	Asphaltene
0.1087 g 100 %	0.0608 g 55.93 %	0.0450 g 41.40 %*	0.0114 g 10.49%*	0.0008 0.74%*	0.0035 3.22%*

Hydrocarbons	Saturates	Aromatics	Resin	Asphaltene
92.82%**	74.07%**	18.75%**	1.39%**	5.79%**

Normal Paraffin	Branched Paraffin	Cyclic Paraffin
70.30%**	11.88%**	17.82%**

* Percentage relative to total oil sample
** Percentage relative to nC9+ recovery

TABLE 8. Range and mean of whole-rock X-ray diffraction analyses of 46 sandstone and 30 shale samples from the upper Almond formation. From Keighin, Law, and Pollastro, 1989[21]

	Shallow core samples (4,500 - 7,500 ft)		Deep core samples (9,600 - 13,700 ft)	
	Sandstone	Shale	Sandstone	Shale
Quartz:				
range	25 - 81	22 - 52	38 - 91	22 - 43
mean	57	37	67	33
Clay:				
range	13 - 25	44 - 67	3 - 26	47 - 72
mean	18	51	18	59
Carbonates:				
range	0 - 55	0 - 19	0 - 42	0 - 31
mean	20	10	12	5
calcite	8	2	3	<1
dolomite	4	5	3	3
ankerite	8	<1	6	<1
siderite	-	<1	<1	1
Feldspar:				
range	0 - 15	2 - 5	0 - 12	1 - 6
mean	5	3	3	3
Pyrite:				
mean	-	2	-	2

TABLE 9. - Mean clay-mineral compositions of sandstone and shale from the upper Almond formation as determined by X-ray diffraction. From Keighin, Law, and Pollastro, 1989[21]

	Shallow core samples (4,500 - 7,500 ft)		Deep core samples (9,600 - 13,700 ft)	
	Sandstone	Shale	Sandstone	Shale
Illite	23	36	44	41
Illite/smectite	30	48	51	47
Kaolinite	47	14	5	9
Chlorite	0	2	0	3

TABLE 10.- Whole rock X-ray diffraction analysis, in weight percent, for samples from Patrick Draw upper Almond formation core samples

Well	Depth, ft	Quartz	Plagioclase	K Feldspar	Calcite	Dolomite	Ferroan Dolomite	Siderite	Pyrite	Kaolinite	Illite/Mica	Illite/Smectite
7-18-1[1]	4,945	61	4	4	3	-	21	-	3	3	1	tr
45-14-3[2]	4,450	5	-	tr	93	-	tr	-	-	2	tr	tr
49-1-3[3]	4,515	69	-	2	1	10	15	-	1	1	1	tr
74-14-6[4]	4,305	78	2	3	5	5	tr	2	1	2	2	tr

[1] Tightly cemented, cross laminated sandstone.
[2] Oyster rubble in silty fine sandstone.
[3] Faintly cross laminated fine sandstone
[4] Ripple laminated sandstone and interbedded mudstone.

TABLE 11. - Permeability reduction of core samples from Patrick Draw field as a result of fresh water injection, after Baptist, White, and Land[37]

Porosity, %	Air permeability, md	Fresh water permeability, md	Ratio of water to air permeability
17.9	[1]30	[1]15	0.5
	[2]26	[2]13	0.5

[1]Arithmetic average for all core samples.
[2]Geometric average for all core samples.

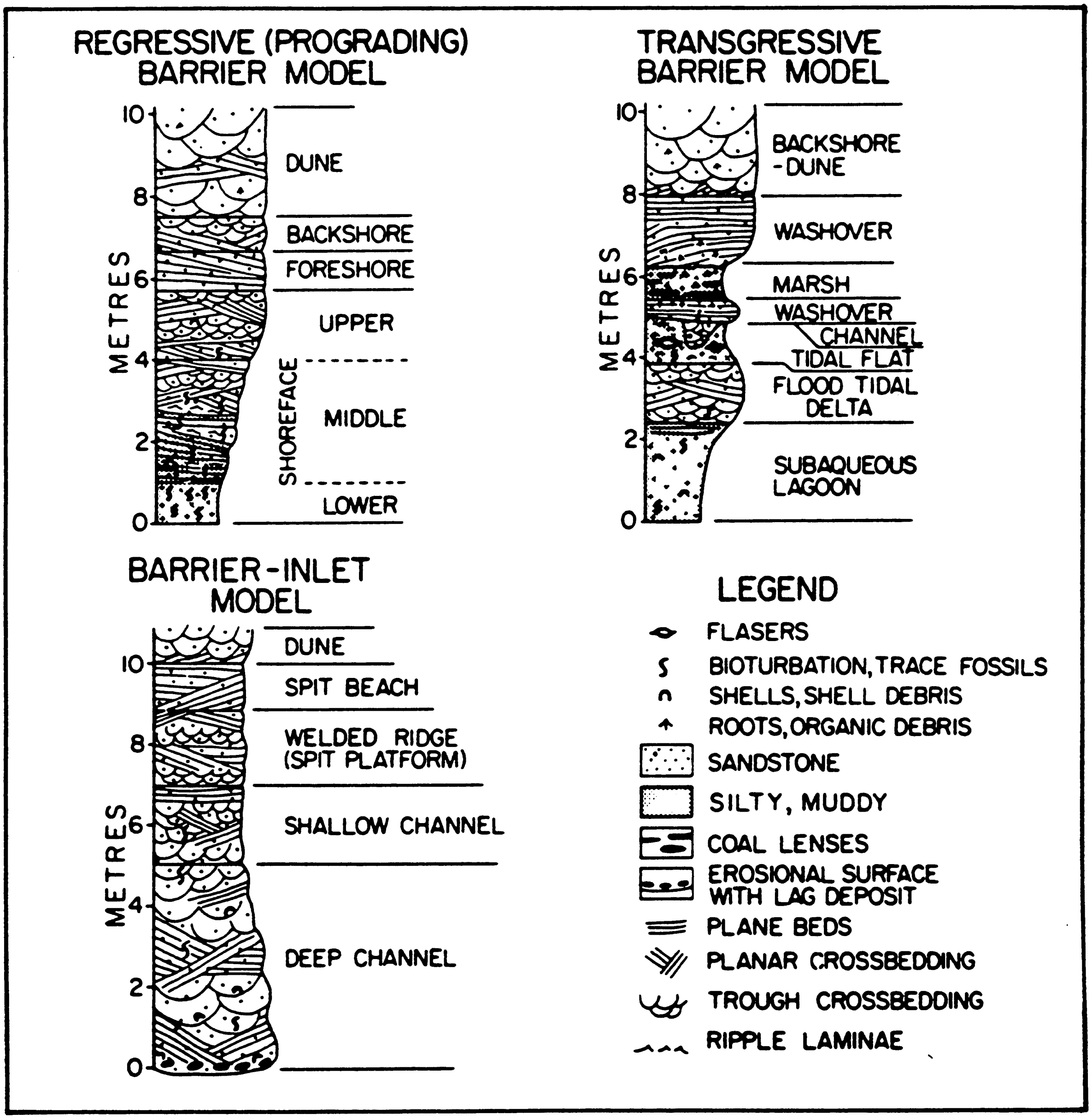

Figure 1. Three "end-member" facies models of barrier island stratigraphic sequences. Although each section has been standardized to 10 m, thicknesses could range up to a few tens of meters. From Reinson, 1979.[1]

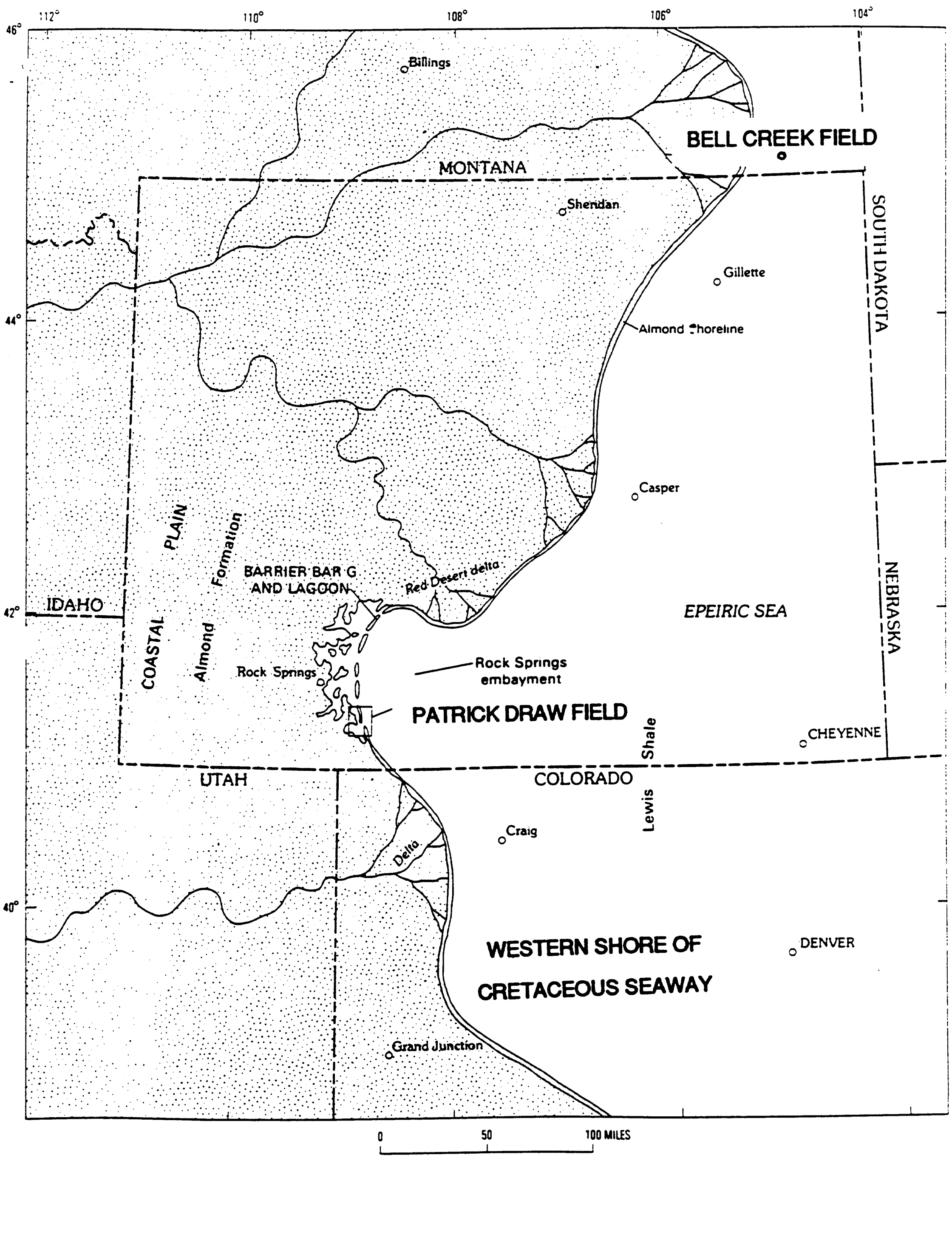

Figure 2. Paleogeographic setting of the Almond formation shoreline/barrier island system on the western shoreline of the Late Cretaceous epeiric sea. After Roehler, 1988.

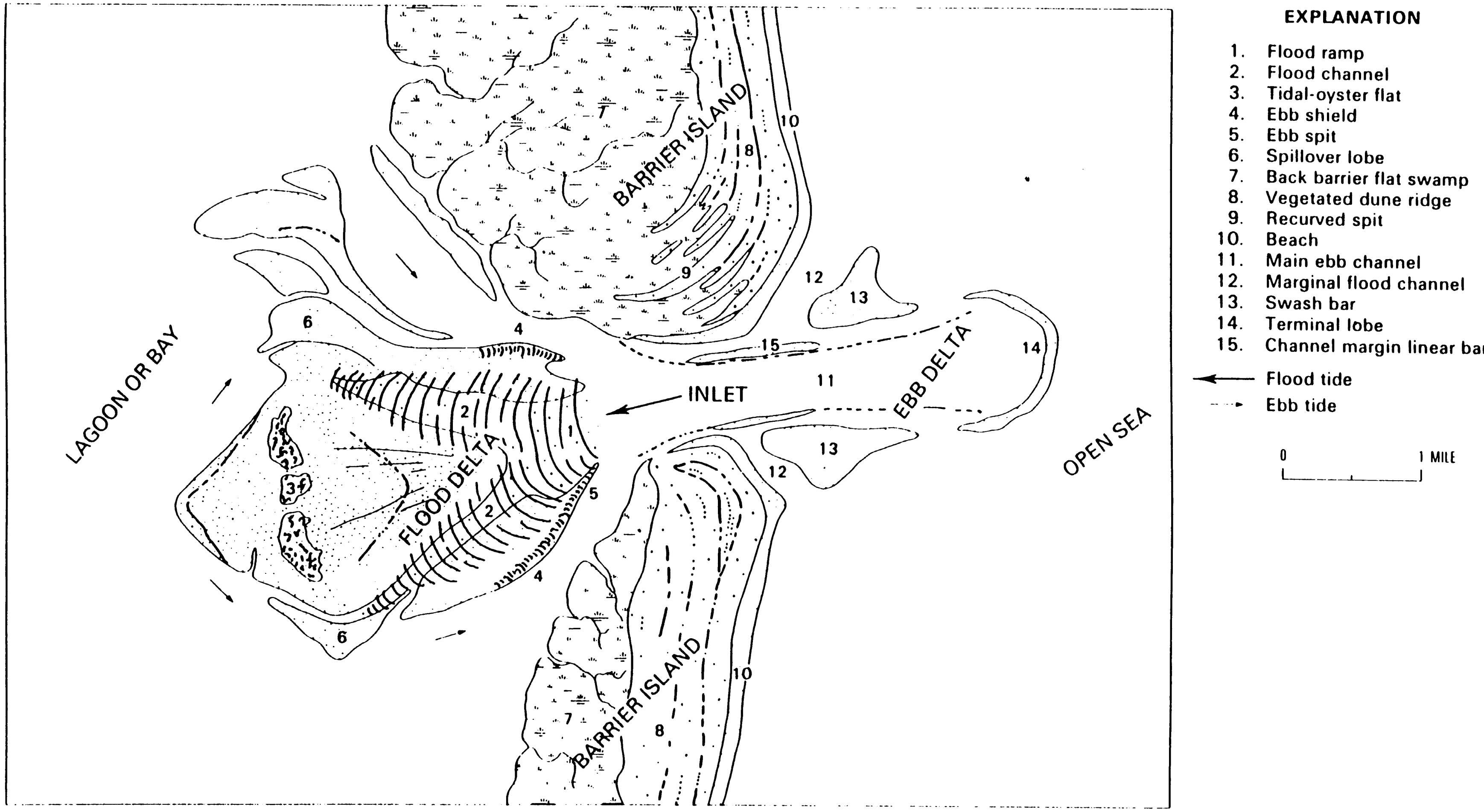

Figure 3. Nomenclature and anatomy of facies deposited in a mesotidal barrier island system. After Hayes and Kana, 1976.[20]

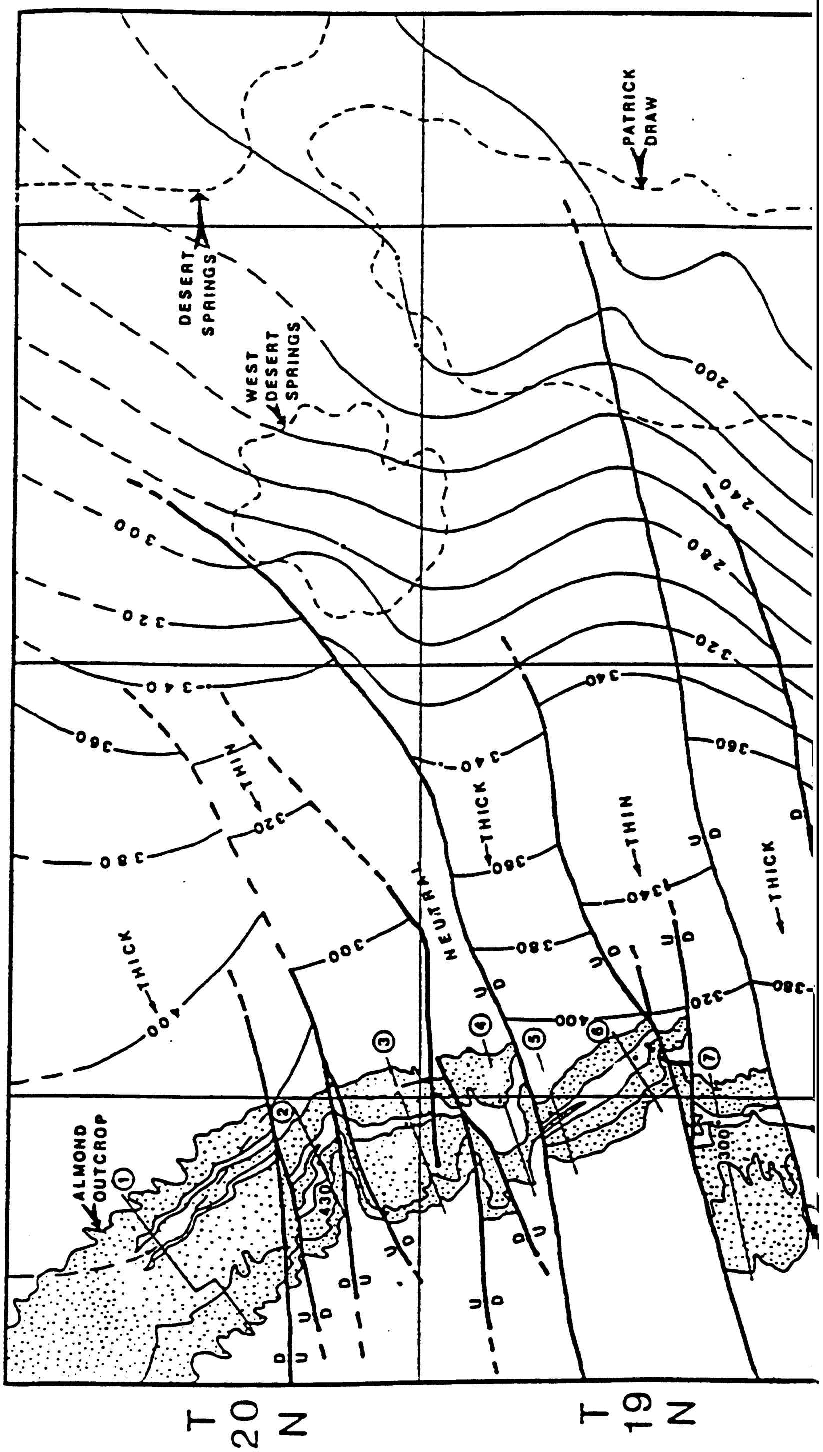
ALMOND OUTCROP
DESERT SPRINGS
WEST DESERT SPRINGS
PATRICK DRAW
THICK
THIN
NEUTRAL
T 20 N
T 19 N
200
240
280
300
320
340
360
380
400
430

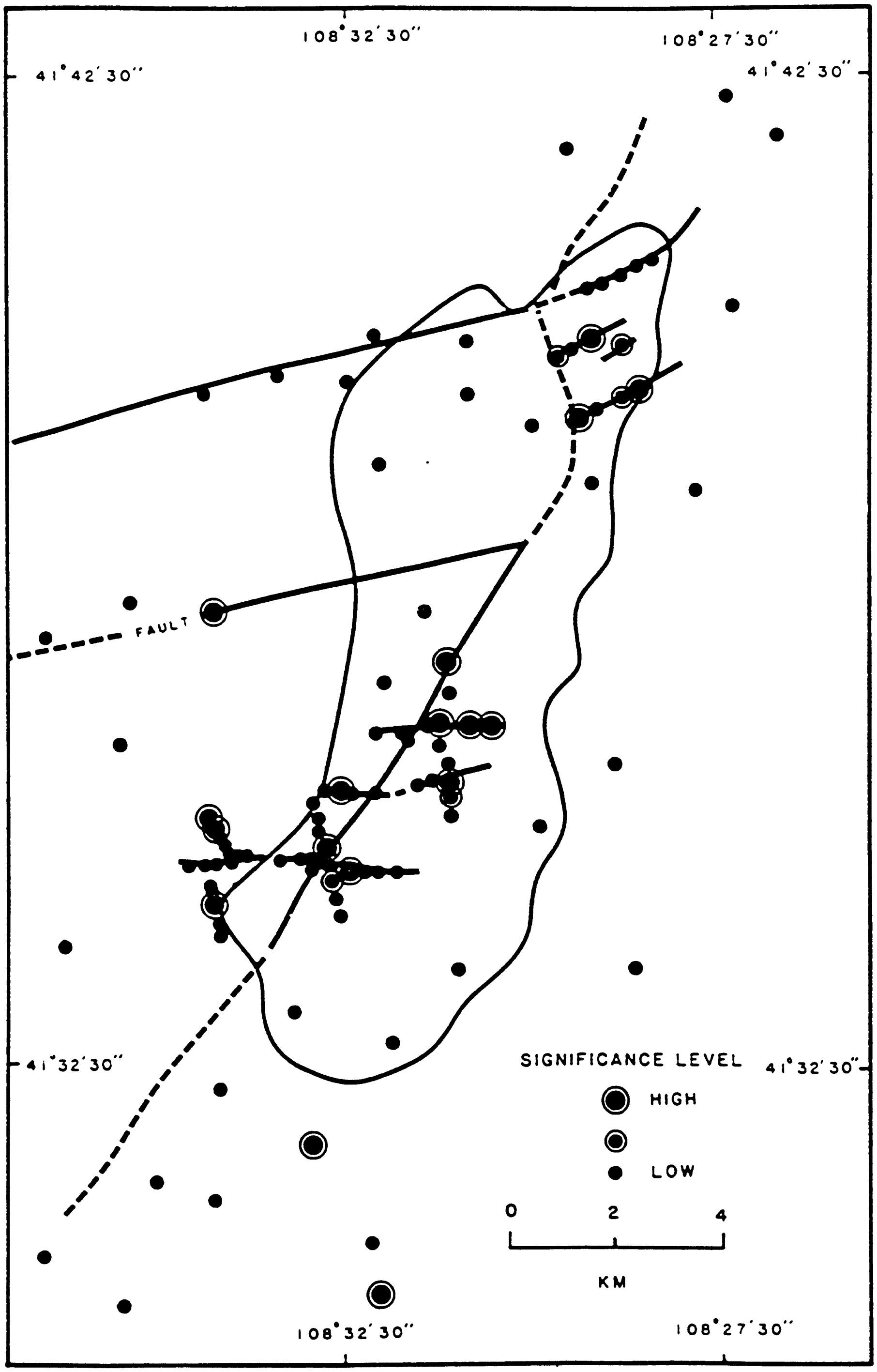

Figure 5. Combined geochemical anomalies and faults at Patrick Draw oil field from the 1980 Geosat study. After Richers, 1982.[27]

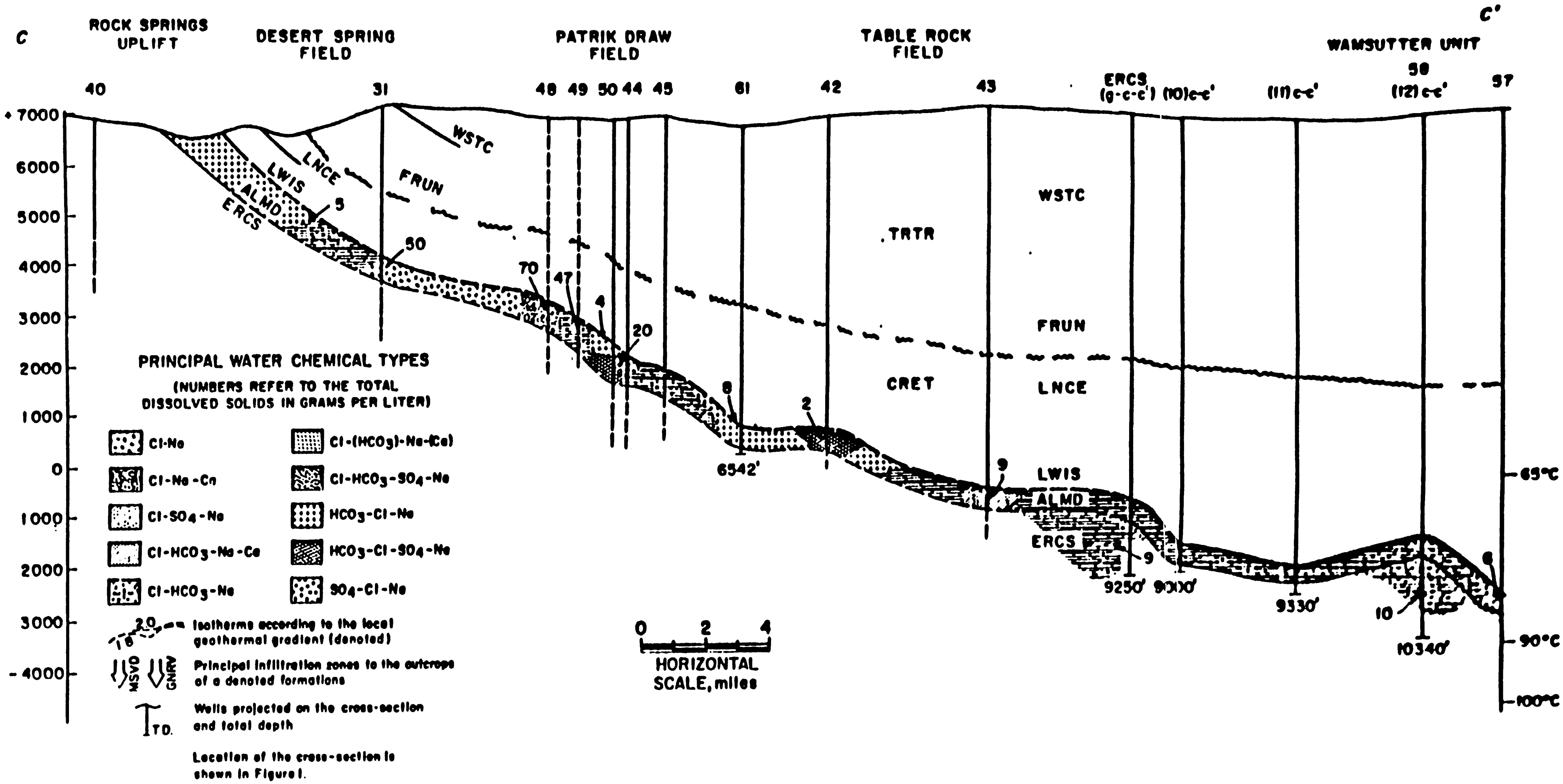

Figure 6. Hydrochemical cross-section east of the Rock Springs Uplift, Greater Green River Basin. Almond formation interpreted. Geology based on the log correlation by Tyler, 1979 (cross section C-C'). After Szpakiewicz and Collins, 1985.

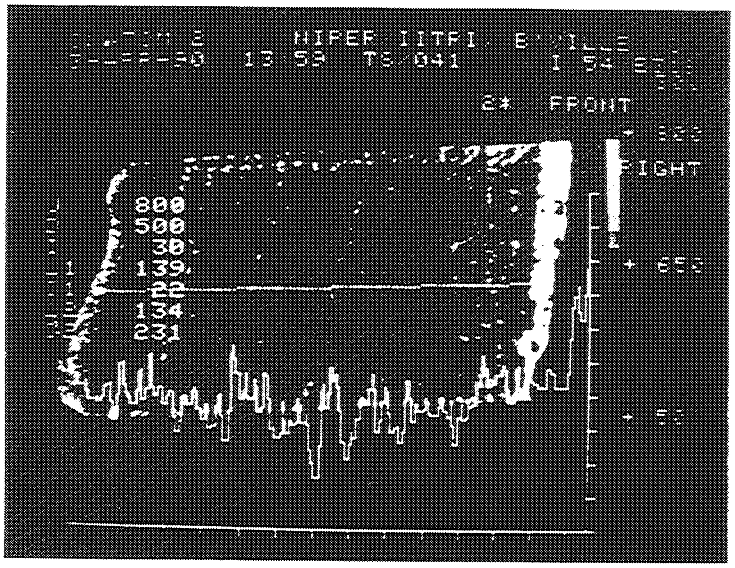

Figure 7. CT scan and density profile for porous,cross bedded sandstone from Patrick Draw field well 49-1-3 at 4,552 ft. CT density varies from about 600 to 700 H.U.

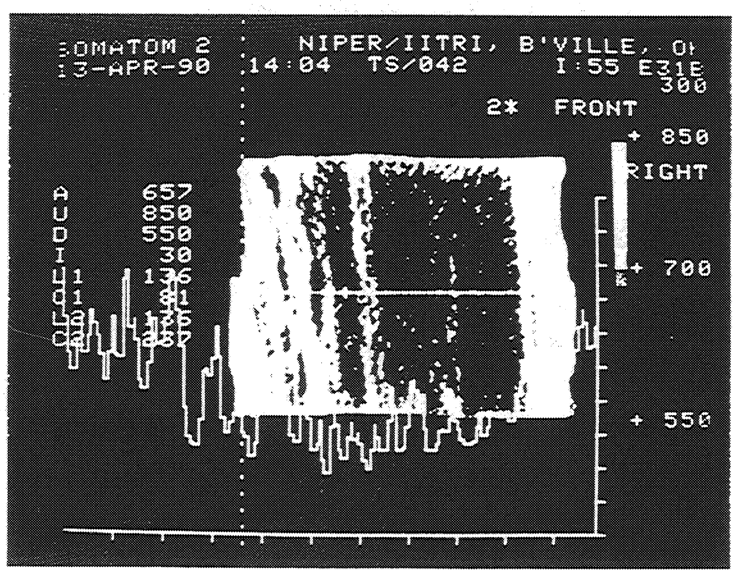

Figure 8. CT scan and density profile for thinly laminated sandstone from Patrick Draw field well 49-1-3 at 4,531 ft. CT density varies from about 650 to 750 H.U.

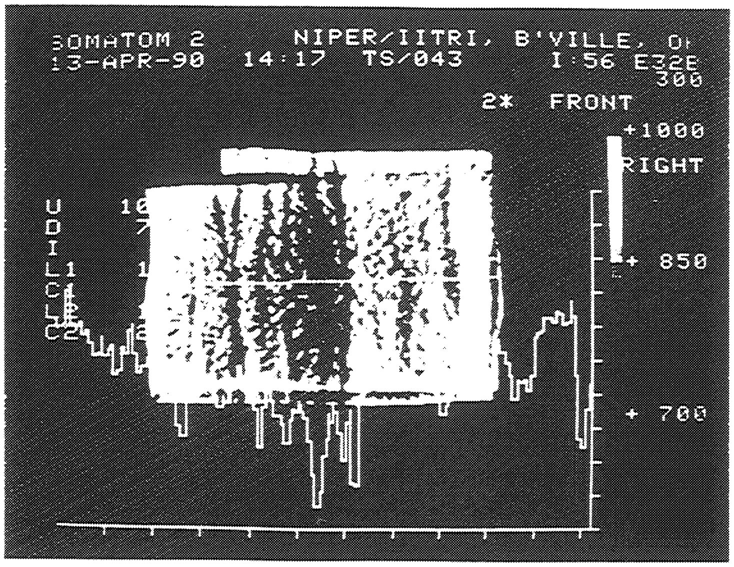

Figure 9. CT scan and density profile for interlaminated silty, very fine sandstone and silty shale from Patrick Draw field well 7-18-1 at 4,957 ft. CT density varies from about 750 to 850.

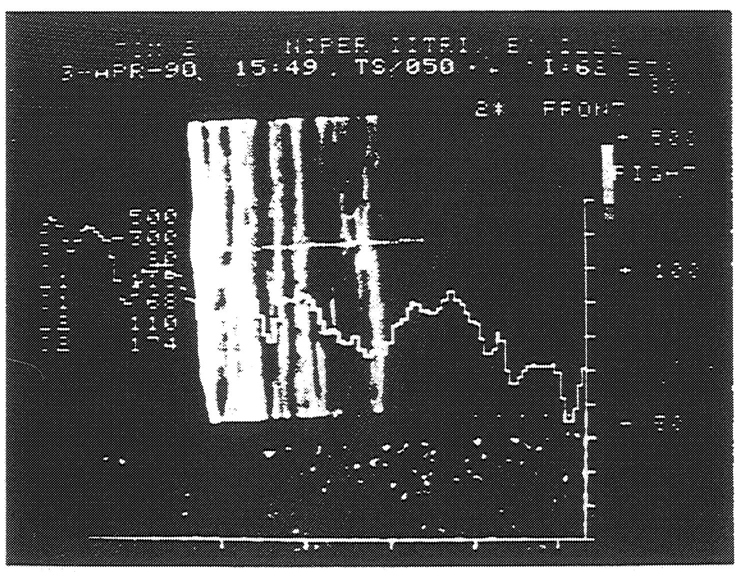

Figure 10. CT scan and density profile for black, coaly siltstone and shale from Patrick Draw field well 78-14-6 at 4,344 ft. CT density varies from 0 to 450 H.U.

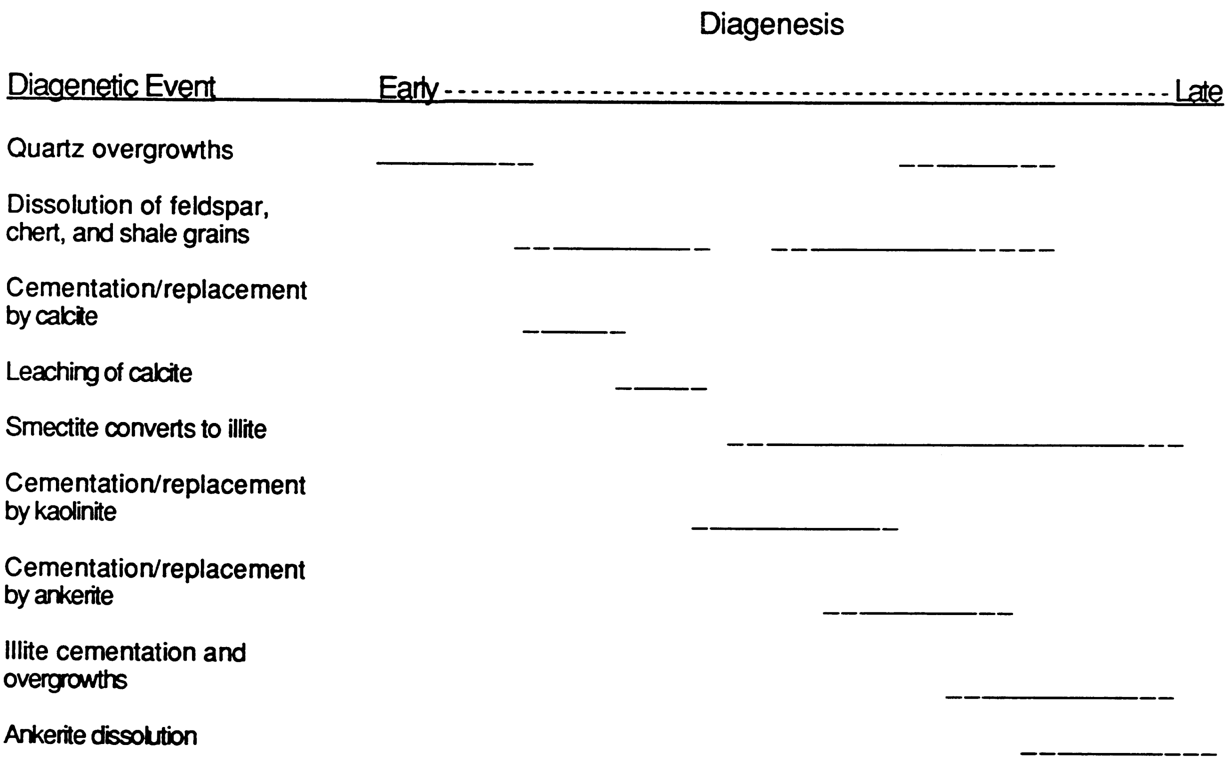

Figure 11. Diagenetic sequence for upper Almond Formation, typical of Patrick Draw field. Modified from Keighin, Law, and Pollastro, 1989.[21]

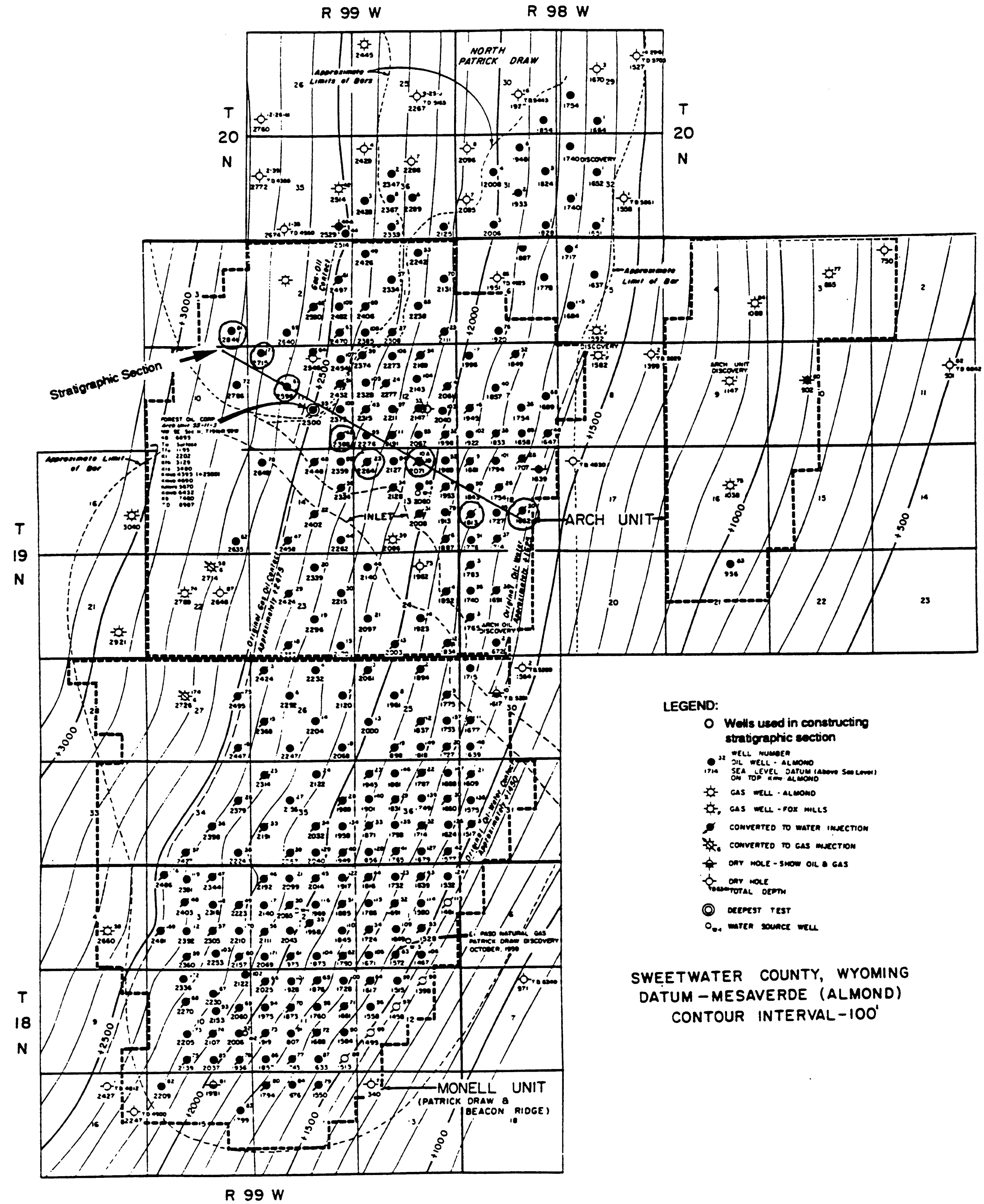

Figure 12. Map showing location of wells within Arch and Monell units of Patrick Draw field and location of log-based dip-oriented stratigraphic section illustrated in fig. 13.

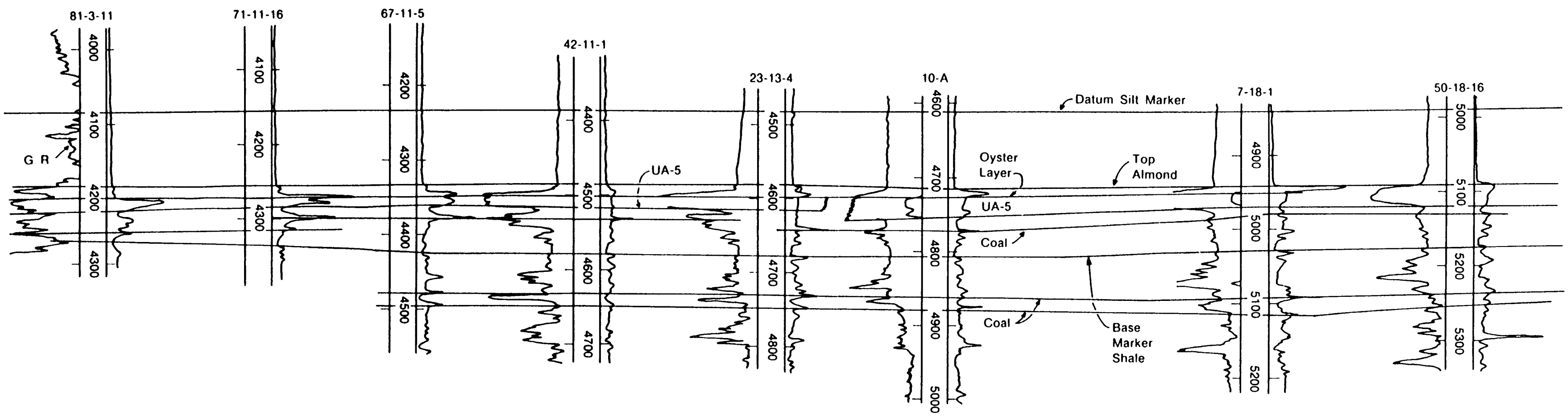

Figure 13. Stratigraphic cross section of upper Almond formation, showing major stratigraphic units. Track 1 (left side) in well 81-3-11 is Gamma Ray, and in all other wells it is SP. Track 2 (right side) in all wells is Induction Log. See fig. 12 for location.

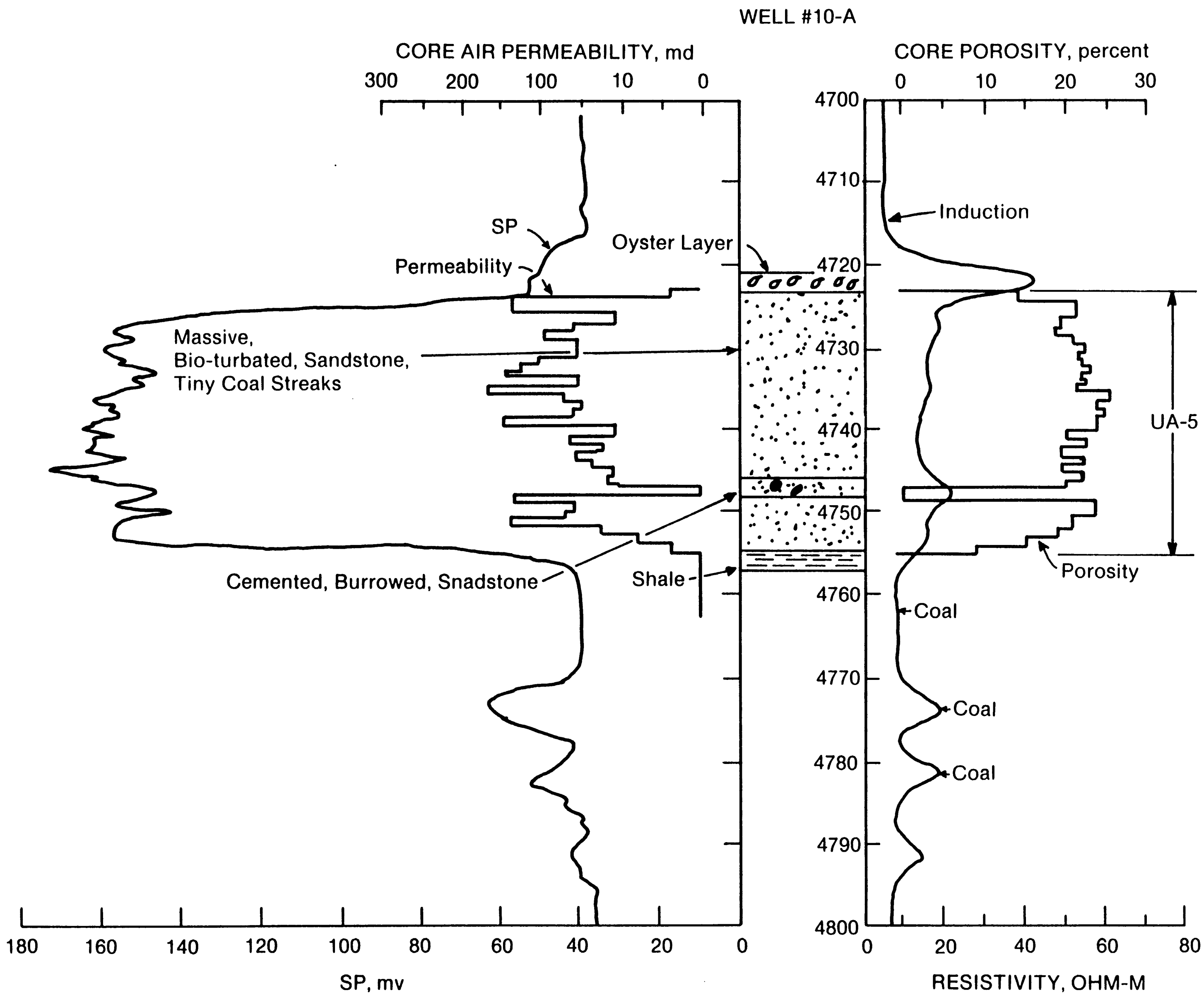

Figure 14. Log responses and petrophysical properties of producing UA-5 sandstone and other geological features of the Upper Almond formation, Patrick Draw field, well no. 10-A. After Union Pacific Resources Office Records.

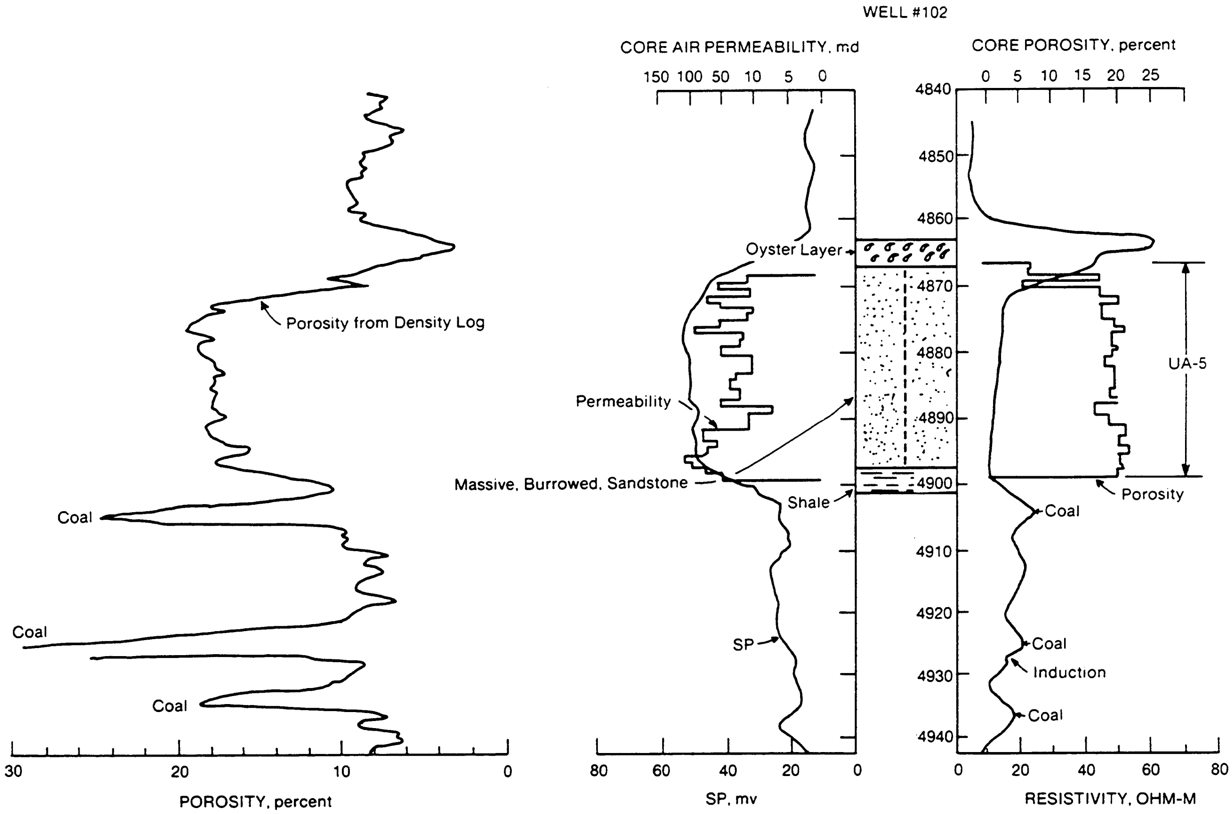

Figure 15. Log responses and petrophysical properties of producing UA-5 sandstone and other geological features in upper Almond formation, Patrick Draw field, well no. 102. After Union Pacific Resources Office Records.

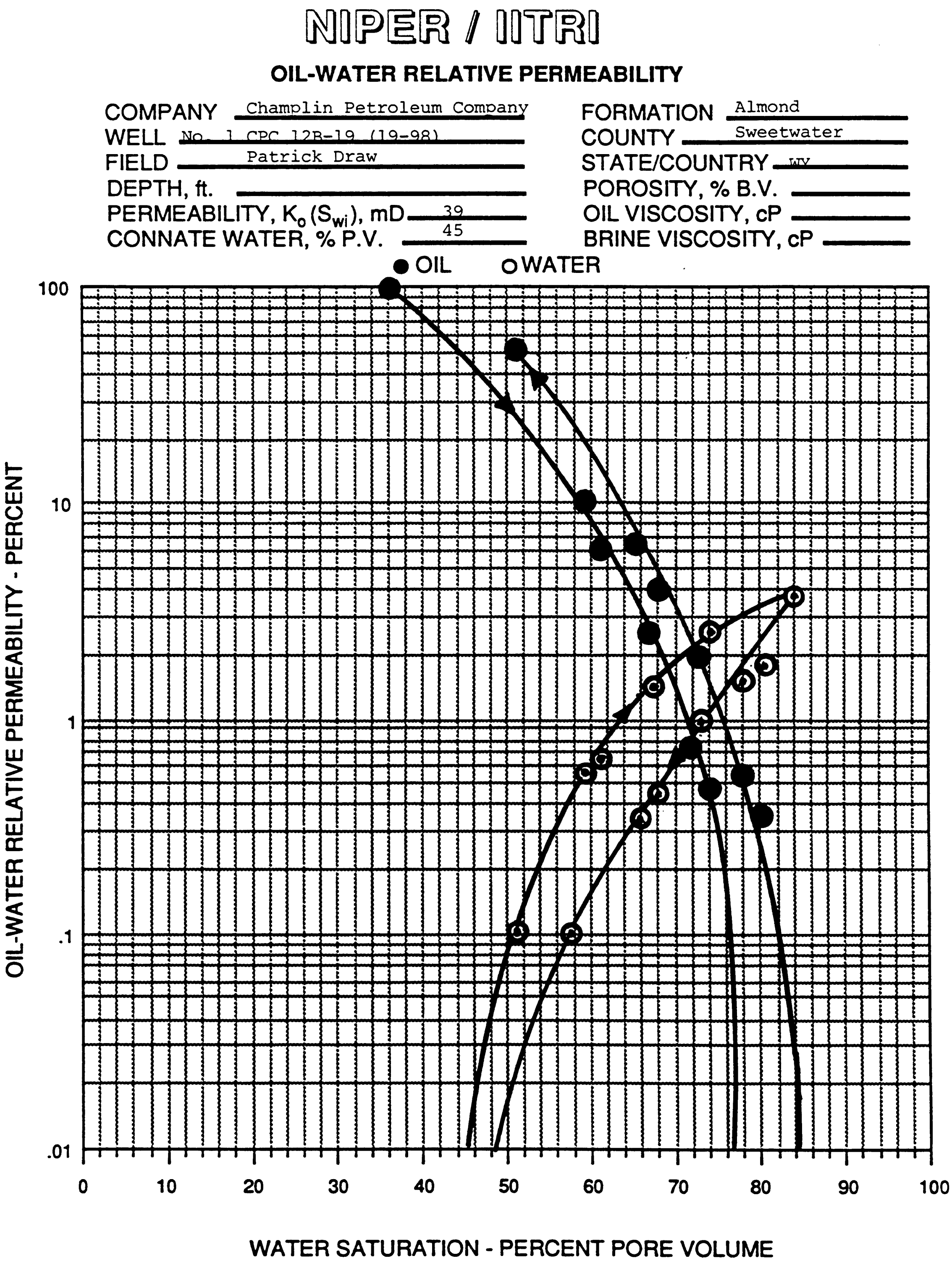

Figure 16. Imbibition and drainage oil-water relative permeability analysis conducted a core sample from the Almond formation at Patrick Draw field. Well identified as Champlin Petroleum Company No. 1, depth unknown.

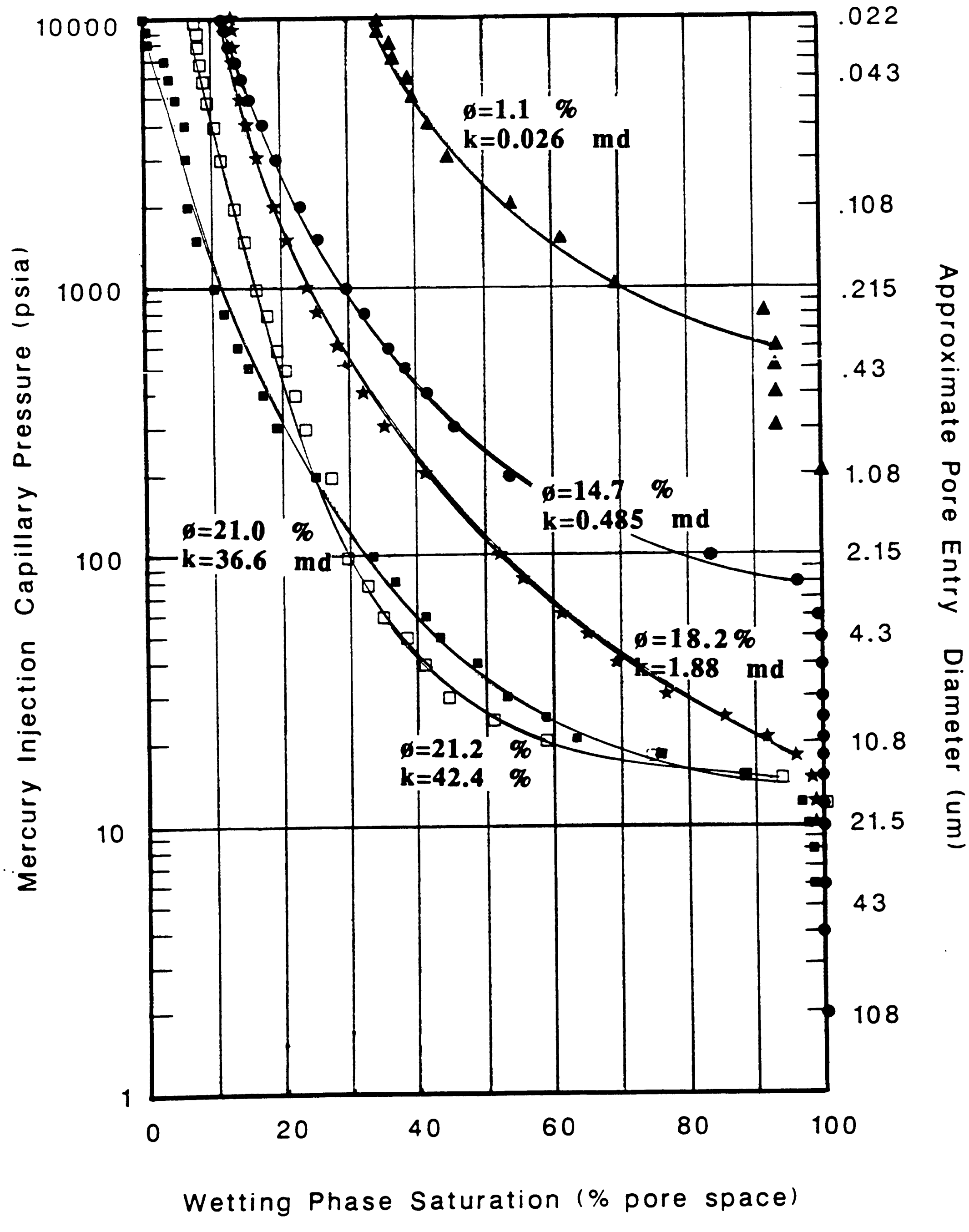

Figure 17. Mercury capillary pressure test results on five core samples from well no. 15, Arch unit, Patrick Draw field. After Keighin, Law, and Pollastro, 1989.[21]

Appendix A. Barrier References and Papers Examined

This appendix provides an example of the information collected during the literature search. The examined literature is tabulated according to major subject (Almond Formation, Patrick Draw Field Studies, etc). Critical statements have been highlighted with bold type. The complete listing, which is available upon request, includes articles examined through April 1, 1990.

ALMOND FORMATION, PATRICK DRAW FIELD STUDIES (by date)

Burton, G., 1961, Patrick Draw Area, Sweetwater County, Wyoming: Wyo. Geol. Assoc., 16th Ann. Field Conf. p. 276-279.

Lawson, D. C., and C. W. Crowson, 1961, Geology of the Arch Unit and Adjacent Areas, Sweetwater County, Wyoming: Wyo., Geol., Assoc. Guidebook, 16th Ann. Field Conf. p. 280-299.

Cox, J. E., 1962, Patrick Draw area, Sweetwater County, Wyoming: Billings Geol. Soc., Paper no. 1, p 1-71.

Weimer, R. J., 1966, Time-Stratigraphic Analysis and Petroleum Accumulation, Patrick Draw Area, Sweetwater County, Wyoming: AAPG Bull., v. 50, p. 2150-2175.

> Field discovered in 1959. Although several sandstone reservoirs produce at Patrick Draw, the principal productive interval consists of two sandstone bars at the top of the Almond formation. Spatial dimensions, lithologic character, and stratigraphic framework of the bars suggest that they are barrier-bar sandstone bodies deposited along the margins of the Lewis sea. The bars are linear and grade updip into impermeable shale and sands that were deposited in a swamp and lagoonal environment. **A second important productive interval is approximately 40 ft below the top of the Almond formation. The areal distribution, lithologic character, and stratigraphic framework of the sandstone in this interval suggest that it was deposited as a tidal delta in a lagoon.** Each of the three major productive ss bodies have different oil-water contacts.

McCubbin, D. G., and M. J. Brady, 1969, Depositional Environment of the Almond Reservoirs, Patrick Draw field, Wyoming: The Mountain Geologist, v. 6, no. 1, p. 3-26.

> Study supports Weimer (1966) that the main reservoir sandstone is a composite shoreline deposit, at least partly replaced updip by lagoonal shales.
>
> **UA-5 at Patrick Draw consists of a "western bar" and a younger "eastern bar" that partly overlaps the western bar.**

The western bar and, in places, the eastern bar rest with sharp contact on a widespread coal that forms the uppermost unit of the underlying cyclic sequence. Both sandstone bodies contain transported bivalves and some forams and show burrows including rare Ophiomorphia. Both sand bodies show a vertical sequence of stratification types interpreted as indicating deposition in nearshore-marine and beach environments on a seaward-prograding shoreline. Lateral changes in stratification types suggest that the seaward direction was to the east. Vertical and lateral variations in grain size record an initial transgression, followed by deposition in progressively more shallow environments during shoreline progradation.

The lagoonal facies that overlies the western bar and appears to be at least partly equivalent to the eastern bar consist of silty to sandy shales and some thin sandstones. Occurrence of large, whole, randomly oriented oyster valves in argillaceous matrix indicates that these oysters are in their original place of growth. Some of the shales contain a microfauna of arenaceous forams. Structures formed by burrowing animals are abundant in the silty or sandy shales.

Appendix B

This appendix contains an example from a spreadsheet that currently contains information from approximately 200 wells. Data concerning well location, core information, total depths and tops of formations, logs available, fluids, and production data are available on the complete listing, which is available on request.

Key for Appendix B

SEC - Section
Tn - Township
RW - Range
LOC - Location
T - Type of core: S-slabbed F-full
MIN. - Minimum depth of core
MAX. - Maximum depth of core
PH - Photographs of core taken
%CR - percentage of core recovered
CQI - Core quality index score
IND - Induction log
ML - Micro log
GR - Gamma ray log
SON - Sonic log
FDL - Formation density log
KB - Kelly bushing
GL - Ground level
IP - Initial production
TOT - Total barrels recovered per 24 hours
% OIL - % oil recovered
PERF - Depths of perforated zones
SH - Shots per foot for perforations
GRAV - Oil gravity, ° API
TD - Total depth
L - Lance formation (Fort Union)
FH - Fax Hill formation
LW - Lewis formation
AL - Almond formation
ER - Ericson formation
ST - Well status
OG - Oil and gas production
WI - Water injection
SP - Surface plug
GI - Gas injection
TA - Temporarily abandoned
A - Abandoned
PA - Plugged and abandoned
O - Oil production
G - Gas production
SI - Shut in
DA - Dry and abandoned
TP - Temporarily plugged (records indicate intention to re-enter well)
GV - Gas vent
ND - Never drilled

Appendix B

	LOCATION							CORE					LOG					ELEVATION		IP						TOPS						
LOC.	SEC	TN	RW	LIB	OPERATOR	NAME	T	MIN	MAX	PH	%CR	CQI	IND	ML	GR	SON	FDL	KB	GL	tot	GAS	%oil	Perfs	sh	grav.	TD	L	FH	LW	AL	ER	ST
SE SW	11	18	99	C810	EL PASO	5 PATRICK DRAW UNIT	S	4978	5015	X	30	30	X	X	X			6720	6708	781		100	4980-5010	4	43.4	5096	0	3532	3718	4980		w l
SE SW	6	19	98	A410	FOREST	76-6-1 GOV ARCH UNIT	S	4898	4948		24	68	X		x	X		6810	6797	15		67	4897-4906	4		5032	2605	3508	3742	4890		SP
NW SE	7	19	98	A412	FOREST	36-7-4 ARCH UNIT	S	5042	5060		14	5	X					6787	6775	180		99.7	5041-5054	4		5425	0	3606	3848	5034	5389	gl
NW NE	7	19	98	B159	FOREST	52-7-7 ARCH UNIT	S	4979	4989	X	39	69	X					6808	6796	40		99.8	5.5"@2460	4		5375	2688	3534	3773	4969	5356	SP
SENW	9	19	98	B538	FOREST	1-9-6 UPRR UNIT	S	5744	5779	X	72	127	X	X				6802	6791	0		0	5728-42	4		6900	0		4374		6056	
SE NW	10	19	98	B177	FOREST	80-10-1 ARCH UNIT	S	5949	6013	X	25	60	X	X				6779	6770	33		66.7	5956-68	4		6200	0	3524	4539	4638	5877	TA
NW SW	18	19	98	B534	FOREST	17-18-1 ARCH	S	4843	4873	X	40.5	75.5	X	X				6763	6750	324		100	4949-4968	4		5208	2524	3528	3840	4943		A
NW NW	18	19	98	A394	FOREST	9-18-2 ARCH UNIT	S	4879	4904		48	70	X					6758	6745	232		100	4884-4899	4		5400		3457	3767	4876		SP
SE NW	18	19	98	B181	FOREST	26-18-3 ARCH UNIT	S	5040	5065	X	25	55	X	X				6797	6784	504		100	5044-5064	4		5447	2637	3620	3927	5037	5409	SP
NE NW	18	19	98	B185	FOREST	101-18-10 ARCH UNIT	S	4998	5028	X	40	55	X		x		X	6784	6772	32		100	5003-5023	4		5090		3568	3849	4993		SP
NW SW	1	19	99	A411	FOREST	60-1-6 ARCH UNIT	S	4553	4604		15	35	X	X				6945	6933	184		98	4592-4602	4		5300	0	3213	3458	4545		
NW NW	1	19	99	B533	FOREST	49-1-3 ARCH UNIT	S	4580	4630	X	25	60	X	X				6990	6978	580		100				4959	0	3240	3457	4570	4919	TA
SE NE	1	19	99	A579	FOREST	70-1-8 ARCH UNIT	S	4790	4815		46	111	X		x	X		6911	6898	66		30	4793-4810	4		4890	2564	3415	3686	4787		SP
SW SW	1	19	99	A396	FOREST	108-1-9 ARCH UNIT	S	4532	4588		28	73	X		x		X	6901	6889	132	237	100	4527-43"64-72	4		4593		3197	3455	4515		SP
SE SE	2	19	99	A393	FOREST	63-2-2 GOV ARCH UNIT	S	4475	4528	X	32	40	X	X				6926	6914	545		100	4484-4496	4			0	3126	3387	4466		w l
NE SE	2	19	99	B182	FOREST	109-2-6 ARCH UNIT	S	4485	4543	X	23	58	X		x		X	6952	6939	115	646	96.5	4523-4533	4		4553		3131	3372	4471		TA
SE SE	3	19	99	B183	FOREST	81-3-1 UPRR ARCH UNIT	S	4205	4256	X	0	30	X		x	X		7025	7012	102		100	4230-4242	4		4286	0	2945	3090	4185		TA
SW NE	8	19	99	B056	FOREST	1-8 GOVERNMENT	S	3485	3539		40		X	X				7114	7103	0						3859		2363	3479	3759		A
SE SE	11	19	99	B175	FOREST	42-11-1 ARCH UNIT	S	4510	4533	X	23	23	X	X				6878	6865	260		99.6	4495-4515	4		4895	0	3148	3367	4489	4843	
NW NW	11		99	A392	FOREST	71-11-6 ARCH UNIT	S	4261	4312		33	93	X		x	X		6965	6952	438		100	4294-4310	4		4370	3014	3177	4257	4370		P*A
NE NE	11	19	99	A409	FOREST	107-11-8 ARCH UNIT	S	4465	4523		27.5	67.5	X		x		X	6904	6892	35		0.86	4497-4505	4		4525		3190	3397	4451		
NE SE	12	19	99	A406	FOREST	103-12-12 ARCH UNIT	S	4774	4808		26	66	X		x		X	6808	6796	38		52.6	4774-4801	4		4808		3327	3610	4769		P*A
SE SW	12	19	99	A391	FOREST	11-12-1 GOV ARCH UNIT	S	4656	4700		21	56	X	X				6845	6833	146		97.6	4671-87"90-93	4		5000		3233	3510	4651		P*A
SE NW	12	19	99	B184	FOREST	106-12-15 ARCH UNIT	S	4630	4688	X	22	77	X		X			6889	6877	10	16.5	70	4633-4674	4		4790		3245	3467	4616		TA
SE NE	12	19	99	B178	FOREST	41-12-5 ARCH UNIT	S	4763	4792	X	25	40	X	X				6814	6803	333		91				5300	0	3345	3602	4758	5116	w l
SE SE	13	19	99	A163	FOREST	6-13-1 ARCH UNIT	S	4858	4894	X	50	70	X	X				6750	6738	684		100	4871-4895	4		5400						w l
NW NE	13	19	99	B179	FOREST	10-A-13-3-ARCH	S	4715	4751	X	0	40	X	X				6790	6778	1100		100	4726-4754	4		5175		3284	3612	4718	5125	P*A
NWNW	13	19	99	B535	FOREST	23-13-4 ARCH	S	4592	4620		27	62	X	X				6848	6835	744		99.7	4596-4616	4		5050		0	3180	3480	4583	O
SE SW	13	19	99	B176	FOREST	39-13-7 ARCH	S	4666	4796		13.6	75	X	X				6750	6740	0	2479	0	4882-4894	4		5100	0	3260	3560	4664	5016	G
SW NE	13	19	99	A413	FOREST	88-13-9 ARCH UNIT	S	4712	4752		34	79	X					6761	6748	261		100	4706-4740	4		4793		3283	3600	4701		P*A
NW NW	14	19	99	B537	FOREST	74-14-6 ARCH UNIT	S	4300	4308	X	22	55																				
NW SE	14	19	99	A388	FOREST	22-14-1 ARCH UNIT	S	4464	4482		28	62	X	X				6856	6847	112		99.7	50.5 "@2000	4		4850		2146	3075	3389	4450	SP
SE SE	14	19	99	A439	FOREST	44-14-2-ARCH UNIT	S	4552	4586	X	30	95	X	X				6821	6808	1264		100				4950	0	3143	3439	4553	4891	O
NW NE	14	19	99	B536	FOREST	45-14-3 ARCH	S	4449	4472	X	23	50	X	X				6895	6882	804		100				4848	0	3110	3308	4446	4800	w l
SE NW	22	19	99	B180	FOREST	74-22-2 ARCH UNIT	S	4155	4207		24	64	X		x	X		6915	6902	0	1123	0	4164-68	4		4300	0	2787	3041	4125		SI
NWNE	23	19	99	S395	FOREST	20-23-4 ARCH UNIT	S	4497	4547				X	X				6828	6815	1578		100	4493-4518	4		4895		3162	3394	4484	4837	SP
SE SW	23	19	99	A581	FOREST	18-23-2 ARCH UNIT	S	4447	4498		23	83	X	X				6804	6791	1752		100	4464-4495	4		4871	2238	3070	3321	4452	4805	SP
SE SW	24	19	99	A414	FOREST	13-24-3 ARCH UNIT	S	4827	4861		20	80	X	X				6830	6818	212		100	4837-4865	4		5300		3476	3720	4826		
SONE	6	19	98	S260	FOREST	86-6-2 ARCH UNIT	F	4906	4925				X		X			6855	6846	0		0				4925	surf.	3520	3722	4904		P*A
NWSW	7	19	98	S261	FOREST	16-7-1 ARCH	F	4828	4859				X	X				6777	6764	1340		100	4837-58	4		5000		0	3451	3699		
NWNW	7	19	98	S262	FOREST	17-7-2 ARCH	F	4836	4860				X	X				6824	6812	360		95	4841-54	4		5300	0	3439	3680	4836	5237	TA
SESE	7	19	98	S263	FOREST	48-7-6 ARCH UNIT	F	5145	5172				X	X	X			6819	6806	252		100				5550	0	3714	3987	5139	5496	SP
NESE	7	19	98	S264	FOREST	68-7-8 ARCH UNIT	F	5103	5149				X		x	X		6806	6793	366			5126-5148	4		5399	0	3653	3922	5118		
SWSW	7	19	98	S265	FOREST	102-7-10 ARCH UNIT	F	4863	4901				X		x		X	6782	6770	30		100	4871-4899	4		4960		3447	3708	4860		SP
NWSE	18	19	98	S266	FOREST	50-18-6 ARCH UNIT	F	5097	5121				X					6765	6752	356		99.8	5.5"@2400	4		5500	3542	3688	3963	5090	5462	SP
NWSW	19	19	98	S268	FOREST	3-19-2 ARCH UNIT	F	4949	5000				X					6733	6725	938		99.8	4967-4990	4		5400			3798	4961	5344	
SWNW	19	19	98	S269	FOREST	96-19-5 ARCH UNIT	F	5001	5003				X				X	6739	6730	27		100	5008-5032	4		5048		3583	3796	5000		SP
NWNE	21	19	98	S270	FOREST	83-21-1 UPRR ARCH	F	5872	5925				X	X				6744	6735	34		88	5870-5884	4		6050		4147	4558	5789		SI
NWSW	30	19	98	S271	FOREST	1-30-4 ARCH UNIT	F	5052	5081				X	X				6738	6725	68		99.8	5116-20"68-78	4		5200	0	3610	3912	5055	5406	
SESE	1	19	99	S272	FOREST	25-1-1	F	4772	4822				X	X				6869	6859	64		95	4772-4785	4		5141		0	3400	3616	4767	
SESW	1	19	99	S273	FOREST	27-1-2 ARCH	F	4627	4649				X	X				6919	6907	31		75	4643-4648	4		5033	0	3302	3506	4623	4985	
NWNE	1	19	99	S274	FOREST	53-1-4 ARCH UNIT	F	4476	4526				X	X				6956	6944	820		99.7				5125	0	3366	3614	4720	5088	
SENW	1	19	99	S275	FOREST	57-1-5 ARCH	F	4648	4700				X	X				6958	6945	200		99.4	4675-4696	4		5030	0	3304	3544	4629	4994	
NWSE	1	19	99	S276	FOREST	65-1-7 ARCH UNIT	F	4725	4776				X					6923	6910	488		99.8	4701-4718	4		4850	0	3332	3548	4695		